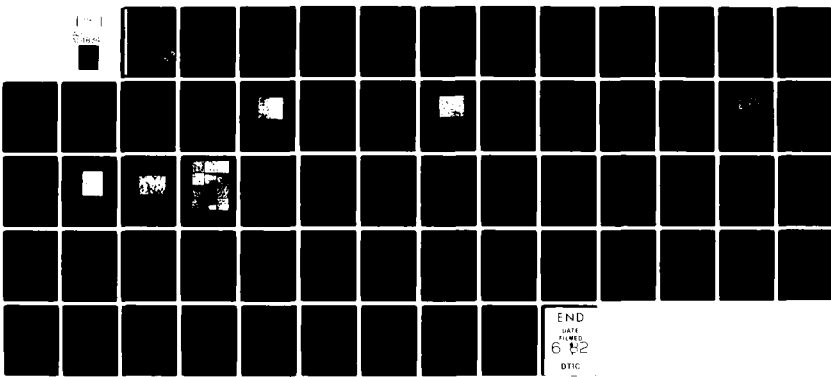


✓ AD-A114 834 MICHIGAN UNIV. ANN ARBOR DEPT OF MATERIALS AND METALL--ETC F/6 11/2
PROCESS DEVELOPMENT FOR SILICON CARBIDE BASED STRUCTURAL CERAMI--ETC(U)
FEB 82 E E HUCKE DAAG46-80-C-0056

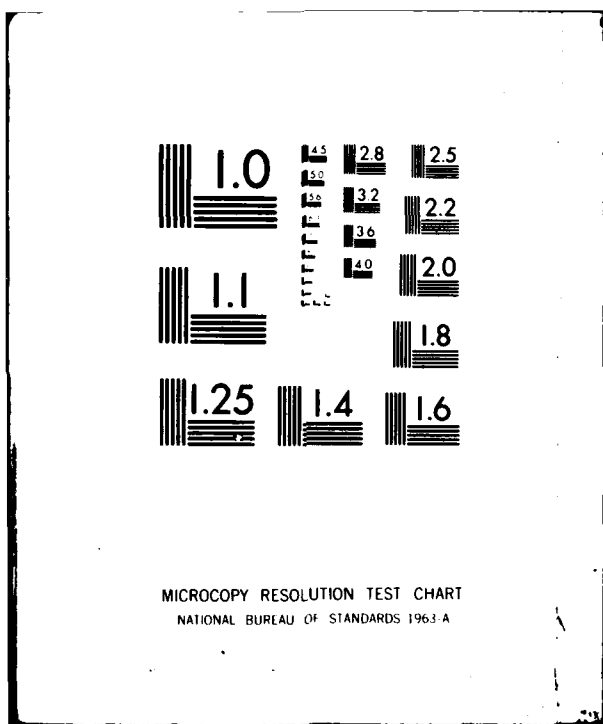
UNCLASSIFIED

AMMRC-TR-82-10

NL



END
DATE
6-4-82
DTIC



12
AU A 114834



AD

AMMRC TR 82-10

PROCESS DEVELOPMENT FOR SILICON CARBIDE
BASED STRUCTURAL CERAMICS

FEBRUARY 1982

Edward E. Hucke, Principal Investigator
Materials and Metallurgical Engineering
The University of Michigan
Ann Arbor, Michigan 48109

Interim Report for Contract No. DAAG46-80-C-0056

Approved for public release; distribution unlimited.

DTIC FILE COPY

Prepared for

ARMY MATERIALS AND MECHANICS RESEARCH CENTER
Watertown, Massachusetts 02172

DTIC
SELECTED
MAY 25 1982
S H

22 05 01 204

Report DAAG46-80-C-0056
AAMRC TR 82-10

PROCESS DEVELOPMENT FOR
SILICON CARBIDE BASED STRUCTURAL CERAMICS

Edward E. Hucke, Principal Investigator
Materials & Metallurgical Engineering
The University of Michigan
Ann Arbor, Michigan 48109

February 1982

Interim Report for Period 1 Jan 1981 - 31 August 1981

Unlimited Distribution

Prepared for

DEFENSE ADVANCED RESEARCH PROJECTS AGENCY
1400 Wilson Boulevard
Arlington, Virginia 22209

Program Code OY10
ARPA Order No. 3906

ARMY MATERIALS AND MECHANICS RESEARCH CENTER
Watertown, Massachusetts 02172

This research was supported by the Advanced Research Projects Agency of the Department of Defense and was monitored by the Army Materials and Mechanics Research Center under Contract No. DAAG46-80-C-0056.

The views and conclusions contained in this document are those of the authors and should not be interpreted as necessarily representing the official policies, either expressed or implied, of the Advanced Research Projects Agency of the U.S. Government.

UNCLASSIFIED

SECURITY CLASSIFICATION OF THIS PAGE (When Data Entered)

REPORT DOCUMENTATION PAGE		READ INSTRUCTIONS BEFORE COMPLETING FORM
1. REPORT NUMBER	2. GOVT ACCESSION NO.	3. RECIPIENT'S CATALOG NUMBER
DAAG46-80-C-0056 (AMMRC TR 82-10)	AD-A444 834	
4. TITLE (and Subtitle) PROCESS DEVELOPMENT FOR SILICON CARBIDE BASED STRUCTURAL CERAMICS	5. TYPE OF REPORT & PERIOD COVERED 1-1-81 to 8-31-81	
7. AUTHOR(s) Edward E. Hucke, Principal Investigator	6. PERFORMING ORG. REPORT NUMBER DAAG46-80-C-0056	
9. PERFORMING ORGANIZATION NAME AND ADDRESS Materials & Metallurgical Engineering Dept. The University of Michigan Ann Arbor, Michigan 48109	10. PROGRAM ELEMENT, PROJECT, TASK AREA & WORK UNIT NUMBERS	
11. CONTROLLING OFFICE NAME AND ADDRESS Defense Advanced Research Projects Agency 1400 Wilson Boulevard Arlington, Virginia 22209	12. REPORT DATE February 1982	
14. MONITORING AGENCY NAME & ADDRESS (if different from Controlling Office) Army Materials and Mechanics Research Center Watertown, Massachusetts 02172	13. NUMBER OF PAGES 60	
	15. SECURITY CLASS. (of this report) Unclassified	
	15a. DECLASSIFICATION/DOWNGRADING SCHEDULE	
16. DISTRIBUTION STATEMENT (of this Report) Approved for public release; distribution unlimited.		
17. DISTRIBUTION STATEMENT (of the abstract entered in Block 20, if different from Report)		
18. SUPPLEMENTARY NOTES		
19. KEY WORDS (Continue on reverse side if necessary and identify by block number) Silicon Carbide Reaction Bonded Silicon Carbide Structural Ceramics Ceramics Ceramic Processing		
20. ABSTRACT (Continue on reverse side if necessary and identify by block number) The objective of this program is to develop a process for making shaped silicon carbide based ceramic materials with reduced microstructural flaw size by in situ reaction of silicon with fine, ultra-uniform pored carbon skeletons that are produced from liquid polymer solutions without particulate additions. Subsidiary objectives are: (1) delineation of the maximum section size producible while maintaining microstructural uniformity; (2) production of microstructures with characteristic features reduced from the current level of approximately 5-10 microns to the level of 1 micron or less; (3) character-		

DD FORM 1 JAN 73 1473 EDITION OF 1 NOV 68 IS OBSOLETE

UNCLASSIFIED

SECURITY CLASSIFICATION OF THIS PAGE (When Data Entered)

Unclassified

Block No. 20

ABSTRACT

ization of microstructure, corresponding strength levels, and statistical uniformity; 4) delineation of dimensional tolerances and surface finish that can be held during processing without finished machining.

Very uniform and reproducible carbon skeletons have been produced and modified to provide for easy siliconization. Complete carbon reaction during siliconization without extensive grain coarsening or formation of silicon veins and/or lakes has been achieved from 1 cm thick samples of carbon skeleton with particle size of 3.2 μm and pore size of 1.9 μm . The siliconized material has a maximum grain size of $<10 \mu\text{m}$ and a Weibull characteristic four point bend strength of 660 MPa, which significantly exceeds other reaction bonded silicon carbide materials and compares favorably with hot pressed SiC (NC203) tested under similar circumstances.

Sections about 6 mm thick which have a maximum grain size $<1 \mu\text{m}$ have been prepared.

micrometers

010
COPY
INSPECTED
2

Accession for
NTIS CR#
DTIC TAS
Unnumbered
Justification

By _____
Distribution/
Availability Codes
Avail and/or
Dist Special

A		
---	--	--

ABSTRACT

The objective of this program is to develop a process for making shaped silicon carbide based ceramic materials with reduced microstructural flaw size by in situ reaction of silicon with fine, ultra-uniform pored carbon skeletons that are produced from liquid polymer solutions without particulate additions. Subsidiary objectives are: 1) delineation of the maximum section size producible while maintaining microstructural uniformity; 2) production of microstructures with characteristic features reduced from the current level of approximately 5-10 microns to the level of 1 micron or less; 3) characterization of microstructure, corresponding strength levels, and statistical uniformity; 4) delineation of dimensional tolerances and surface finish that can be held during processing without finished machining.

Very uniform and reproducible carbon skeletons have been produced and modified to provide for easy siliconization. Complete carbon reaction during siliconization without extensive grain coarsening or formation of silicon veins and/or lakes has been achieved from 1 cm thick samples of carbon skeleton with particle size of 3.2 μm and pore size of 1.9 μm . The siliconized material has a maximum grain size of <10 μm and a Weibull characteristic four point bend strength of 660 MPa, which significantly exceeds other reaction bonded silicon carbide materi-

materials and compares favorably with hot pressed SiC (NC203)
tested under similar circumstances.

Sections about 6 mm thick which have a maximum grain size
 $<1 \mu\text{m}$ have been prepared.

SUMMARY

The objective of this program is to develop a process for making shaped silicon carbide based ceramic materials with reduced microstructural flaw size by in situ reaction of silicon with fine, ultra-uniform pored carbon skeletons that are produced from liquid polymer solutions without particulate additions. Subsidiary objectives are: 1) delineation of the maximum section size producible while maintaining microstructural uniformity; 2) production of microstructures with characteristic features reduced from the current level of approximately 5-10 microns to the level of 1 micron or less; 3) characterization of microstructure, corresponding strength levels, and statistical uniformity; 4) delineation of dimensional tolerances and surface finish that can be held during processing without finished machining.

Very uniform and reproducible carbon skeletons have been produced and modified to provide for easy siliconization. Complete carbon reaction during siliconization without extensive grain coarsening or formation of silicon veins and/or lakes has been achieved from 1 cm thick samples of carbon skeleton with particle size of 3.2 μm and pore size of 1.9 μm . The siliconized material has a maximum grain size of $<10 \mu\text{m}$ and a Weibull characteristic four point bend strength of 660 MPa, which significantly exceeds other reaction bonded silicon carbide materi-

materials and compares favorably with hot pressed SiC (NC203) tested under similar circumstances.

Sections about 6 mm thick which have a maximum grain size $<1 \mu\text{m}$ have been prepared.

TABLE OF CONTENTS

	PAGE
ABSTRACT	3
SUMMARY	5
INTRODUCTION	8
EXPERIMENTAL RESULTS	14
Carbon Skeleton Development	14
Siliconization	21
PROPERTY EVALUATION	31
Indentation Testing	31
Strength Testing	44
CONTINUING WORK	59
Carbon Skeleton	59
Siliconization	59
Property Evaluation	60

INTRODUCTION

The current development program is aimed at providing silicon carbide based high temperature structural ceramics with more reproducible strength properties than those now available. The present understanding of failure mechanisms in well designed ceramic parts clearly identifies maximum flaw size and frequency as performance limiting. Current ceramics with generally satisfactory properties contain processing flaws that severely limit mechanical performance. These flaws are due to: 1) the material's microstructural variation, and 2) surface finishing or damage from other external load concentrations.

In a detailed study of seven commercial silicon carbide materials¹ microstructural flaws were found to limit strength at room temperature in all but one material, a hot pressed grade (NC203). In the latter case, rough machining apparently caused relatively severe subsurface strength limiting defects. The other materials studied included four reaction bonded grades and two sintered varieties. The microstructural flaws that limited strength were occasional large SiC grains and/or agglomerates, silicon lakes and/or veins, large carbon or other inclusions, or porosity.

Due to the inherently low fracture toughness of ceramics (3-8 MPa·m^{1/2}), the processing requirements are intensified

¹Characterization of Turbine Ceramics After Long-Term Environmental Exposure, G. D. Quinn, AMMRC TR 80-15, April 1980.

since for the contemplated design stresses the largest tolerable defect is less than 100 microns. This is smaller than readily detectable with current non-destructive evaluation methods. In the better ceramics now available, the limiting defects are 30-250 microns, even though these materials typically possess average microstructural features in the range 10 microns or less. It is, therefore, necessary to attack processing variables responsible for the occasional larger defects, and to simultaneously develop a processing means for providing complex shapes with smooth surfaces requiring little or no rough finishing.

A detailed rationale and explanation of the approach adopted in the current program was given previously². This approach seeks to avoid the problems of residual porosity, local composition control, and exogeneous inclusions which arise from the crushing, mixing, dispersion, and molding of abrasive micron sized powder systems. This is accomplished by casting the desired shape from filterable low viscosity polymerizable liquids devoid of any particulate fillers. The liquids, after casting and polymerization, may be further shaped by machining and are then pyrolyzed to a fine and very uniform carbon skeleton. The skeleton parameters, such as maximum carbon particle size, degree of carbon crystallinity, pore size, and pore volume, are

²Process Development for Silicon Carbide Based Structural Ceramics, AMMRC TR 81-13, Dec. 1980, E. E. Hucke, Principal Investigator.

controlled by simple chemical means (time, temperature, concentration) and not by the mechanical variables in mixing, dispersion, and molding of powders. The carbon is subsequently reacted in situ with silicon in a manner similar to several commercial reaction bonded silicon carbides.

There are several distinctions between the current approach and other self bonded silicon carbides, where in most cases the silicon reacts with a carbon bonded skeletal body which already contains a large fraction of particulate solids, such as α -silicon carbide and/or carbon. While in some cases the particulate has a relatively fine size ($\sim 10 \mu\text{m}$) there are always much larger agglomerates present which cause occasional large micro-structural features, such as silicon lakes, large silicon carbide grains or unreacted carbon.

The carbon skeletons for this program are being developed so as to have no carbon solids larger than $5 \mu\text{m}$; spatially uniform and selectable pore volume; very narrow pore size distribution; high hot strength; and low real density.

For reasons that are not well understood, the in situ reaction of silicon with a porous carbon body whose overall carbon concentration is less than $.963 \text{ gm/cm}^3$ does not usually result in a volume change. This allows shaped bodies with good surfaces to be made accurately to dimension by control of the original carbon shape. However, for bodies with lower carbon concentration, there is residual silicon left in the pores of the body. Table I shows the calculated composition resulting

TABLE I CALCULATED COMPOSITION

Assumptions: $\rho_{Si} = 2.3 \text{ gm/cm}^3$ $\rho_{SiC} = 3.21 \text{ gm/cm}^3$
 Complete reaction of carbon to SiC
 No volume change upon reaction and complete
 filling of pores with Si
 ρ_a is skeleton apparent density
 ρ is the density of the fully reacted body

ρ_a gm/cm ³	Vol% Si	Vol% SiC	Wt% Si	Wt% SiC	ρ gm/cm ³	Wt Si Gained Wt C reacted
.963	0.00	100.00	0.00	100.00	3.205	2.33
.950	1.350	98.65	0.972	99.03	3.193	2.36
.940	2.388	97.61	1.724	98.28	3.183	2.39
.930	3.427	96.57	2.482	97.52	3.174	2.41
.920	4.465	95.53	3.148	96.85	3.165	2.44
.910	5.504	94.50	4.010	95.99	3.155	2.47
.900	6.540	96.46	4.779	95.22	3.146	2.50
.890	7.580	92.42	5.556	94.44	3.136	2.52
.880	8.619	91.38	6.336	93.66	3.127	2.55
.870	9.657	90.34	7.121	92.88	3.118	2.58
.860	10.696	89.30	7.911	92.09	3.108	2.61
.850	11.734	88.27	8.705	91.30	3.099	2.65
.840	12.773	87.23	9.505	90.50	3.089	2.68
.830	13.811	86.19	10.308	89.69	3.080	2.71
.820	14.849	85.15	11.117	88.88	3.071	2.75
.810	15.888	84.11	11.932	88.07	3.061	2.78
.800	16.926	83.07	12.750	87.25	3.052	2.82
.790	17.965	82.10	13.566	86.43	3.044	2.86
.780	19.003	81.00	14.404	85.60	3.033	2.89
.770	20.042	79.96	15.239	84.76	3.023	2.93
.760	21.080	78.92	16.078	93.92	3.014	2.97
.750	22.118	77.88	16.967	83.03	3.005	3.01
.740	23.157	76.84	17.773	82.22	2.995	3.05
.730	24.195	75.81	18.628	81.37	2.986	3.09
.720	25.234	74.77	19.489	80.51	2.976	3.13
.710	26.272	73.73	20.356	79.64	2.967	3.18
.700	27.310	72.69	21.227	78.77	2.958	3.23

from in situ reaction with carbon skeletons of varying carbon concentration, ρ_a .

An accurate control of overall carbon concentration is necessary for control over the residual silicon, which is normally about 10 wt%. However, the local carbon concentration may vary quite significantly from the average which causes large silicon lakes and large silicon carbide grains.

The skeletons in this program have a macroscopically uniform carbon concentration within $\pm 1\%$ and are microscopically uniform on a scale of about 2-3 times the maximum carbon particle size². The structure also has a very uniform pore size which is comparable to the maximum particle size. This feature is essential to the control of the siliconization reaction. If even a few large pores are present, silicon can be delivered rapidly deep within the body which causes a large liberation of reaction heat and drastic thermal gradients along the path of easy access. This results in silicon veins and silicon carbide grain coarsening from solution-precipitation during the temperature excursion.

The formation of silicon carbide from carbon involves a significant increase in volume as a given carbon particle goes from its volume of $.446 \text{ cm}^3/\text{gm}$ (graphite) to $1.038 \text{ cm}^3/\text{gm}$ in silicon carbide.

²Process Development for Silicon Carbide Based Structural Ceramics, AMMRC TR 81-13, Dec. 1980, E. E. Hucke, Principal Investigator.

This expansion of 132 vol.% must be accommodated within the pores of the skeleton if the body does not crack or expand. If the original carbon particle is disordered (true density 1.45 gm/cm³) rather than graphitic, the expansion necessary is only 50.5 vol.% and is far more easily accommodated locally. Therefore, the bodies employed are non-graphitic.

Several important advantages accrue from using a very fine particle size. First, the rate of reaction will not be effectively limited by diffusion through a reaction layer if the solid particle size is fine enough (<10 μm). This insures complete reaction and that no large carbon particles can remain as flaws. Secondly, the local rearrangement required is much easier. For example, a 2 μm diameter disordered carbon particle need only grow to 2.3 μm diameter for complete reaction to silicon carbide. The chances of expanding into an adjacent pore are much better than for a 200 μm particle that must expand to 230 μm thereby disrupting the structure over a much larger distance. The very fine particle and pore size may cause too rapid reaction unless the silicon access to the reacting interface is limited by fluid flow through the skeleton and reacted layer. Such limitation can be achieved with uniform pores of <1 μm provided the skeleton does not crack. With fine enough pores, the reaction should become more nearly isothermal and yet be capable of reacting sections of the order of 1 cm thickness in times of the order of 1 hour.

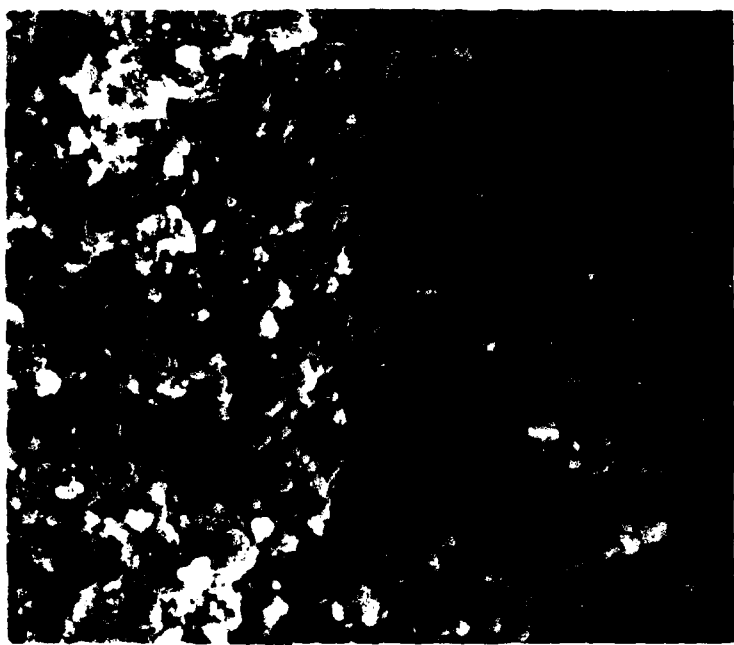
Examples of cracking and subsequent severe thermal spikes causing exaggerated grain growth were previously noted².

EXPERIMENTAL RESULTS

Carbon Skeleton Development

In the initial efforts to experimentally establish the best range of skeleton parameters two widely differing carbons were selected². The coarsest (Fig. 5) had a mercury intrusion pore size of about 2.5 μm with an average particle size of about 6 μm as determined microscopically from the mean linear intercept. However, there were some intercepts ranging up to 20 μm . Some of these larger carbon areas were not completely reacted except with high temperature ($\sim 1550^\circ\text{C}$) siliconization or prolonged holding of about 10 hours at 1450°C ². Neither alternative is attractive due to concurrent microstructural changes such as general coarsening of the silicon carbide. Therefore, a large number of trial carbon batches were prepared with slightly altered polymerization times and temperatures, which resulted in a reduction in the carbon particle size while holding the pore size approximately constant. The average particle size was reduced to 3.2 μm and the average pore size to about 1.9 μm . Moreover, the largest particle size was well below 10 μm . Figure 1 shows a scanning electron micrograph of this material

²Process Development for Silicon Carbide Based Structural Ceramics, AMMRC TR 81-13, Dec. 1980, E. E. Hucke, Principal Investigator.



—

10 microns

Figure 1. Scanning Electron Microscope of Modified Coarse Skeleton (331-2B).

(330-2B) while Fig. 2 shows its mercury intrusion curve. The intrusion volume indicated in Fig. 2 above the plateau (at about 60%) is due to specimen compressibility and not to filling of very fine pores. This was established by using the high pressure data to calculate the compressibility of the carbon which agreed closely with that measured on bulk samples. The narrow pore size distribution was retained.

The finer material (Fig. 7) used originally showed a pore size of .027 μm (Hg intrusion) and a particle size well under .1 μm . The microscopic determination of the particle and pore size becomes very inaccurate for such fine material since the surface roughness even on a polished surface is more than 1 particle size and therefore a photograph does not really represent a plane passing through the structure. This carbon structure gave difficulties in uniformly maintaining a fine structure during siliconization. In the areas where it did not overheat and crack, the silicon carbide grain size was well below 1 μm , but it frequently showed areas with grain size $>1000 \mu\text{m}$ ⁽²⁾. In these cases numerous silicon veins were also noted. For this reason, a second series of carbon batches was prepared in an effort to raise the pore size to about .3 μm . Figure 3 shows SEM micrograph of the resulting carbon (330-10A), while Fig. 4 shows its mercury intrusion curve. The average pore diameter is about

²Process Development for Silicon Carbide based on Structural Ceramics, AMMRC TR 81-13, Dec. 1980, E. E. Hucke, Principal Investigator.

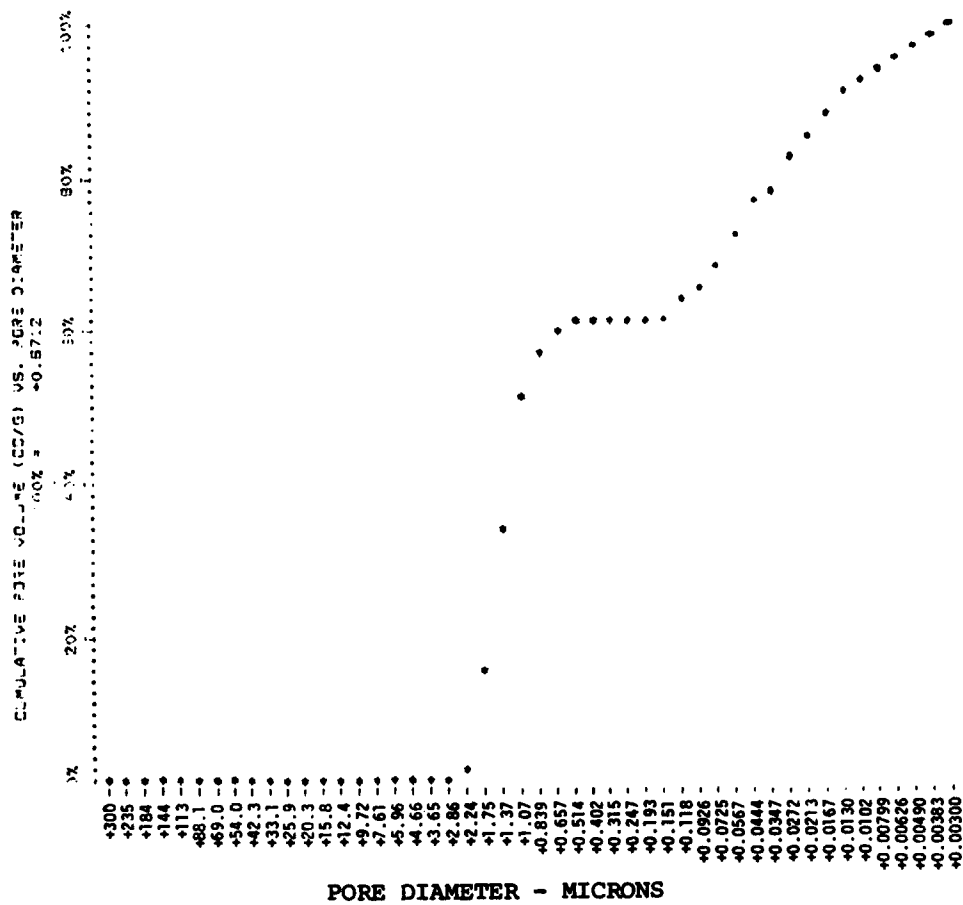
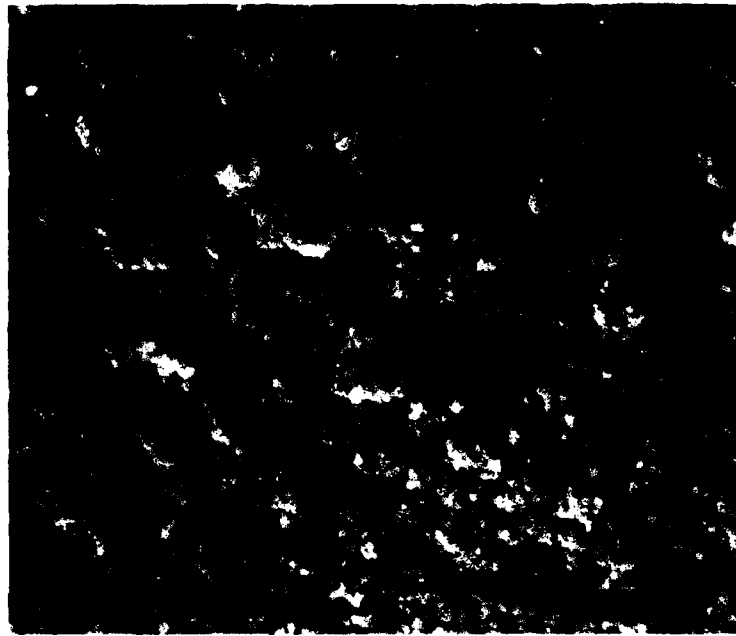


Figure 2. Mercury Intrusion Plot for a Modified Coarse Skeleton (331-2B).



—
10 microns

Figure 3. Scanning Electron Micrograph of Modified Fine Skeleton (331-10A).

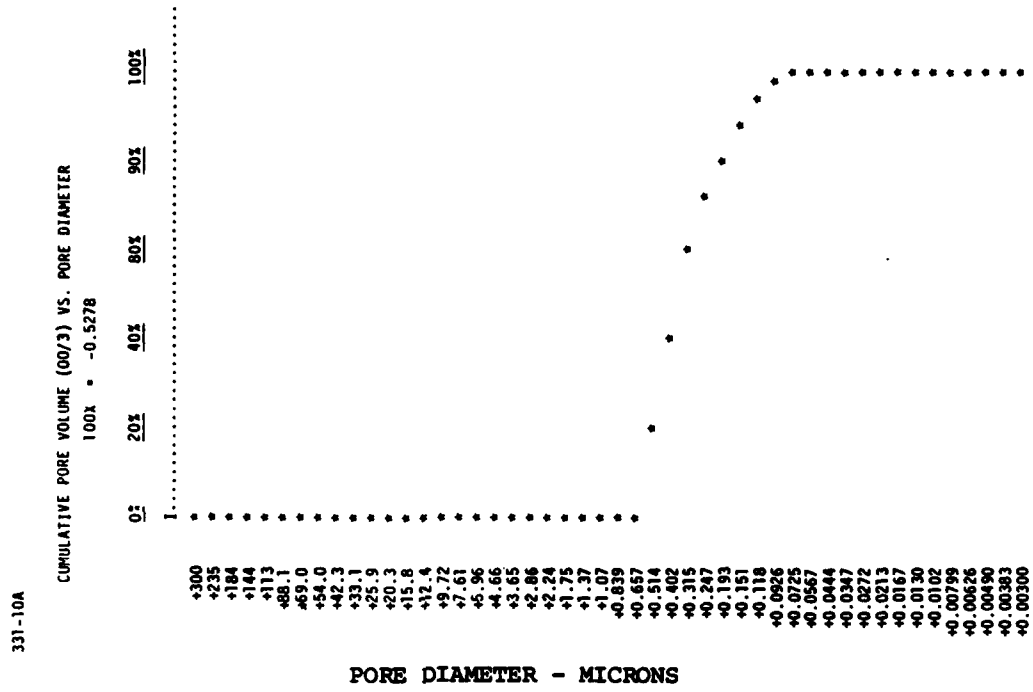


Figure 4. Mercury Intrusion Plot for a Modified Fine Skeleton (331-10A).

It has thus been demonstrated that the skeleton parameters can be "fine tuned" by trial-and-error over wide ranges.

The real density of the disordered carbon comprising the solid part of the skeleton was determined on 14 different carbon variants by mercury porosimetry and xylene pycnometry. The average value for xylene absorption was $1.453 \pm 0.059 \text{ gm/cm}^3$ while for mercury it was $1.420 \pm 0.044 \text{ gm/cm}^3$. The agreement is very good and indicates that all the porosity is open to liquid intrusion.

A curious difference in the final carbon concentration (apparent density) was previously noted between $\sim 2 \text{ cm}$ diameter cylinders and larger blocks cast from the same polymer batch². A lengthy investigation into this phenomenon revealed (fortunately) that it was not due to an inherent size or shape effect, but was related to the mold material. Polymer mixtures cast in either glass or copper molds show $\sim 10\%$ greater final density than those cast in previously used silicone rubber molds. In the former cases, there was a small shrinkage that occurred just after polymerization. In well-used rubber molds, the cast stuck slightly to the rubber and did not undergo this initial shrinkage and, therefore, ended with a slightly lower apparent density.

²Process Development for Silicon Carbide based on Structural Ceramics, AMMRC TR 81-13, Dec. 1980, E. E. Hucke, Principal Investigator.

Control of overall skeleton shrinkage prior to siliconization is not only important for composition control (carbon concentration) but also in order to exactly reproduce complex shapes. While the exact linear shrinkage varies with carbon type between 18-32%, the reproducibility for a given batch type is very good. Seven replicate batches showed a linear shrinkage of $29.1 \pm .6\%$. The variation noted is approximately at the level of error in the dimensional measurement used. This reproducibility can probably be further improved but is already comparable to dimensional control possible in good metal casting processes.

The carbon skeletons can be machined to high tolerance but are somewhat brittle and subject to machining scratches. The unpyrolyzed polymer is easier to machine, giving smoother surfaces and less brittle behavior. Therefore, investigation of distortion during pyrolysis of machined thin test bars was undertaken. Sections ~2 cm thick show no easily measurable distortion. However, groups of transverse test bars ~2 mm square by 60 mm long cut at random locations from larger casts showed significant distortion. About one third of the bars showed warp along the bar in at least one direction of $>.125$ mm. Additional efforts are underway to determine the exact cause of this distortion and to better control the pyrolysis conditions.

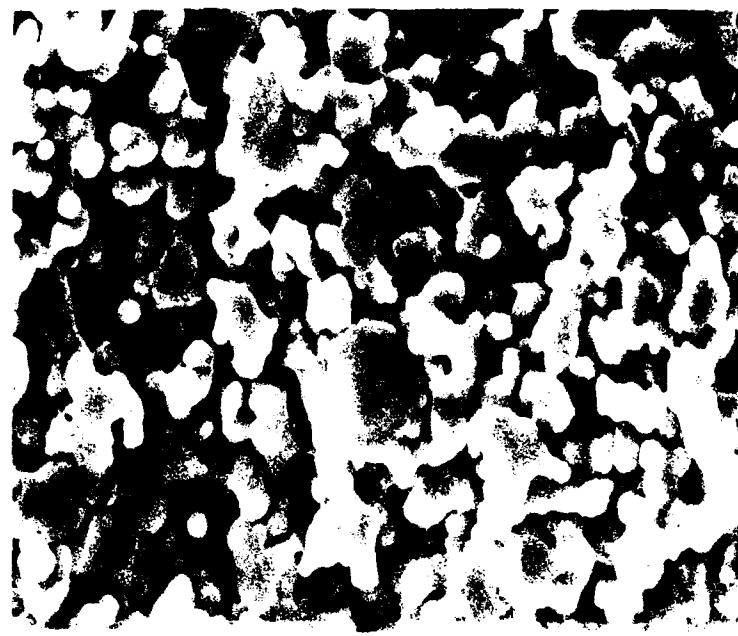
Siliconization

The major problems previously encountered in siliconization have been: 1) minor amounts of unreacted carbon particles, 2) areas of silicon carbide grain coarsening, and 3) silicon

veins. Considerable progress in controlling each of these problems has resulted from adjusting the carbon skeleton parameters. Trial siliconization has been carried out on test coupons ~1 cm thick from each carbon variant.

Earlier trials on the coarsest skeletons gave regions just under the surface where small amounts of carbon was not reacted. These particles were less than 10 μm in diameter and never constituted a major fraction of the structure. With those skeletons, shown in Fig. 5, it was necessary to raise the siliconization temperature to 1550°C or to hold for about 10 hours at 1450°C to avoid all traces of unreacted carbon. The former alternative coarsened the entire structure although not drastically. The second alternative caused only a minor amount of coarsening in the inner portion of the sample but gave a perceptible coarsening and silicon enrichment at the surface. This layer, shown in Fig. 6, was not present in samples held for short times (1-2 hours) and is undoubtedly caused by the continued supply of silicon to the surface. Fortunately the problem of unreacted carbon has been eliminated by lowering the maximum carbon particle size from about 20 μm (Fig. 5) to below 10 μm as shown in Fig. 1. Even the shortest reaction time used (~30 minutes) at 1450°C shows no residual carbon when maximum size falls at or below that in Fig. 1.

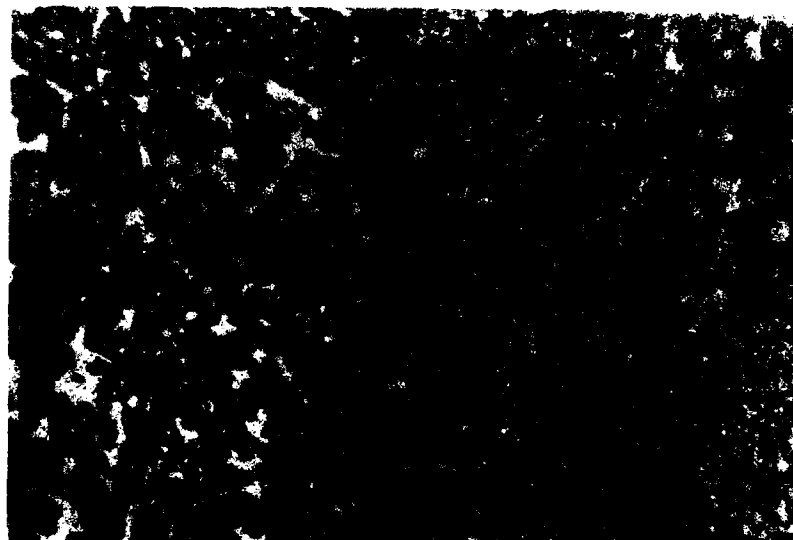
Adjusting the skeleton parameters has aided significantly in minimizing silicon carbide grain coarsening and silicon



—

10 microns

Figure 5. Scanning Electron Micrograph of Skeleton 330-38.



| — |
40 microns

Figure 6. Edge Region (right) on a Reacted Sample (331-34)
Showing Surface Coarsening due to continued supply
of liquid silicon to the surface.

veins. Both problems are aggravated by temperature excursions due to rapid release of the heat of reaction. In the finest skeletons, typified by Fig. 7, exaggerated coarsening often takes place in some portions of the sample (near the center) while the structure remains very fine in adjacent regions². The severe heating and resultant thermal expansion causes the adjacent fine-grained regions to rupture forming silicon filled veins. The overheated regions coarsen severely as shown in Fig. 8. In extreme cases the entire sample overheats and no fine-grained regions remain. In carbons as fine as those in Fig. 7 (~.03 μm pore size), it has thus far been impossible to consistently produce fine grains throughout the entire sample even though some cross sections show only fine grains. However, by increasing the pore size by one order of magnitude (~.3 μm), to a structure shown in Fig. 3, it has been possible to avoid exaggerated silicon carbide coarsening. This also avoids growth of silicon lakes and veins.

The dramatic effects of carbon skeleton variables are best illustrated with a side-by-side comparison of four skeleton types together with the resulting siliconized structures. This collage is presented in Fig. 9 where all structures are shown with a magnification of 1000X. Each row represents a carbon skeleton with varying size, the coarsest at the top and the

²Process Development for Silicon Carbide based on Structural Ceramics, AMMRC TR 81-13, Dec. 1980, E. E. Hucke, Principal Investigator.

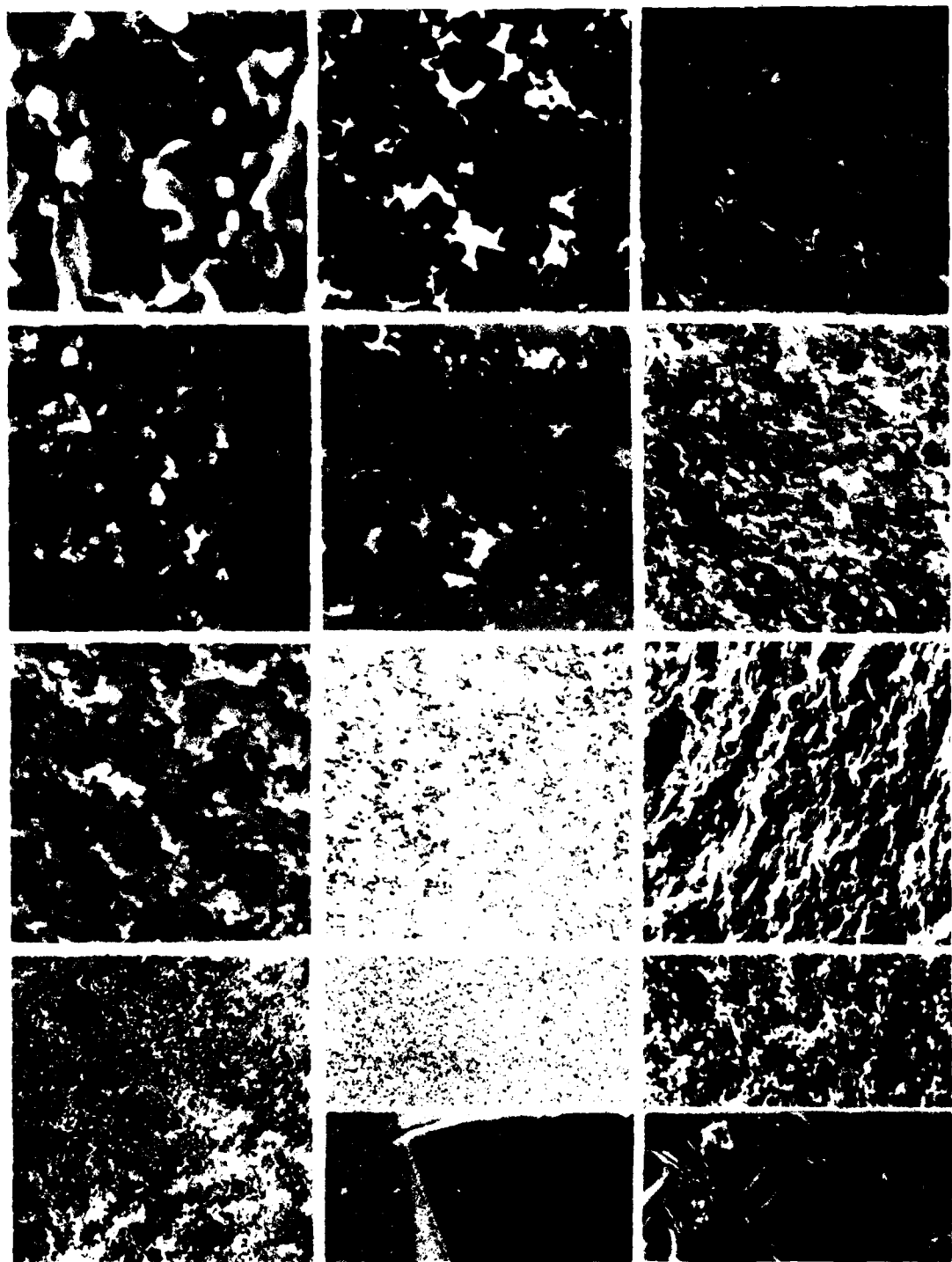


1 micron

Figure 7. Scanning Electron Micrograph of Very Fine Carbon Carbon Skeleton (330-58).



Figure 8. Exaggerated Grain Growth in Center Regions of Sample (330-64) from Very Fine Skeleton.



| — | 10 microns

Figure 9. Effect of Carbon Structure on Reacted Structure. All structures shown at $\sim 1000X$. The columns from left to right are: Carbon skeleton; Polished surface of siliconized body. For the finest skeleton in the bottom row typical and exaggerated growth regions are shown.

finest at the bottom. The columns are respectively, from the left: SEM view of the carbon skeleton, optical view of the reacted material, and SEM view of a fracture surface in the siliconized material. In the last row the reacted structures are split showing both the typical fine grained areas as well as the areas where severe grain growth has occurred. The siliconization in all cases was carried out at about 1450°C for about 5 hours. It is quite evident from Fig. 9 that the scale of final structure parallels that of the carbon skeleton.

In a sample about 8 mm thick of the finest skeleton, it was possible to clearly see the fluid flow limitation at work. After a short time (~15 minutes) at 1450°C, the sample (329-53) was reacted to a very fine grained structure to a uniform depth of ~3 mm from all surfaces. In this case, the skeleton density was relatively high, .867 gm/cm³, and there was no cracking of the fine grained structure. For the coarser skeletons complete reaction proceeds throughout a 1 cm cross-section in the shortest time studied. However, for the most part, the skeleton densities were about .85 gm/cm³ and fluid flow limitation may come into play for high densities where the volume of flow channels drops rapidly (see Table I).

An effort has been made to develop an accurate, routine measure of the residual silicon content. This important variable is usually quoted in "the range of 10 wt%" but is known to vary by a factor of two macroscopically within commercial materials. Chemical attack with various HF acid solutions

removes most of the silicon with little attack of the silicon carbide and, therefore, offers an opportunity for quantitative analysis. However, some of the silicon may be locked in pores with very difficult access for the acid, especially in the structures where the residual silicon channels are $< 1 \mu\text{m}$. Microscopic analysis by point count becomes inaccurate for the fine structures which can barely be resolved optically and where the sampled area becomes very small. Encouraging results have been obtained using an external standard x-ray diffraction technique as outlined by Cullity³. In this method the intensity of lines of a phase α , I_α , in a mixture of α and β phases is compared to the intensity of lines in pure α , $I_{\alpha p}$. The theoretically defined curve has shown agreement to within about 1 wt% Si with mechanical mixed samples of known silicon composition in the range up to ~15 wt% silicon. All samples were crushed to about 325 mesh and a standard area exposed to x-rays. The crushed samples should expose a representative cross-section of silicon carbide and silicon. The intensity was measured 4 times for both the unknown mixture and pure silicon with a typical reproducibility of ~1% in counts. Thus far, only one sample (321-2B) has been studied where accurate carbon concentration, microscopic point count, and x-ray data are available. The results for silicon volume % were respectively, 10, 11, and 10.7, as determined by x-ray, point count, and calculation according to

³B. P. Cullity, Elements of X-Ray Diffraction, 2nd Ed., Addison-Wesley, 1978, p. 407-419.

Table I. Additional refinement should afford a useful tool for correlation of properties to silicon content.

PROPERTY EVALUATION

Property characterization is underway for representative materials. Preliminary screening of materials is on the basis room temperature strength, fracture toughness and hardness. Since this is a substantial expense involved in obtaining test specimens with suitable surface preparation, indentation analysis is being used as a comparative tool. Materials with interesting room temperature properties are to be evaluated by a stepped high temperature stress rupture test.¹

The properties thus far measured should be regarded as preliminary since in each case considerable evolution in procedure and equipment has taken place.

Indentation Testing

Previous research^{4,5} has shown the feasibility of using indentation measurements to quantitatively rank materials with respect to fracture toughness and brittleness as well as hardness.

¹Characterization of Turbine Ceramics After Long-Term Environmental Exposure, G. D. Quinn, AMMRC TR 80-15, April 1980.

⁴Fracture Toughness Determinations by Indentation, A. G. Evans and E. A. Charles, J. Amer. Ceramic Soc. 59, July-August 1976, p. 371-372.

⁵Hardness, Toughness and Brittleness: An Indentation Analysis, B. Lawn and D. B. Marshall, J. Amer. Ceramic Soc. 62, August 1979, p. 347-350.

However, a good deal of attention must be paid to experimental detail in order to yield significant data.

Even in the case of hardness wide discrepancies are noticeable in values reported for very hard materials. Most of the discrepancy results from reporting light load (<1 Kg) results where the Vickers hardness is usually much higher than with heavier loads. However, for very hard materials like SiC even at ~1 Kg the hardness impression is only ~25 μm across and therefore measuring errors are large. Usual criteria⁶ separate the microhardness range from low load hardness range at impression dimensions >30 μm . Indentation analysis is in many ways ideal for comparing mechanical properties of developmental materials. This is due to the ability to probe materials properties on a scale that is larger than that of the microstructure but smaller than the occasional microstructural or machining defects. These latter defects completely dominate larger scale mechanical properties and allow good comparisons only with relatively large numbers of tests with carefully prepared samples.

In the Vickers indentation the impression depth is $.404a$ where a is the half diagonal of the impression. For impressions with $2a = 25 \mu\text{m}$ the depth is only ~5 μm which is just comparable to the average structural size in premium materials. However,

⁶Progress in Microhardness Indentation, H. Buckle, Met. Rev. 4:13, 1959.

it has been shown⁷ in SiC that the radius of the zone of plastic deformation is about 5a or about 63 μm which is large enough to insure sampling a representative structure but with minimal chance of encountering defects. Such defects usually result in an abnormal crack pattern around the indentor and are easily rejected. Thus the data derived can be considered to be representative of the local microstructure. In work carried out to date the zone of plastic deformation is from ~50-200 μm .

The analysis is carried out using a variety of loads with several impressions at each load. Careful measurement of the impression diagonals and the length of the median cracks that emanate from the impression corners is required⁴. Early attempts to use SEM pictures for measurement were unsatisfactory due to the difficulty of maintaining a stable magnification calibration. With a skilled operator the impression, 2a, can be reproducibly determined optically within about 1 μm . The reproducibility in reading the crack length, 2c, is about 5 μm with most of the uncertainty arising from location of the crack tips.

Replicate impressions are required since there may be microstructural variation over the sampled volume, a hemisphere

⁷Indentation Plasticity and Microfracture in Silicon Carbide, J. Lankford, D. L. Davidson, J. Mat. Sci. 14, July 1979, pp. 1669-1675.

⁴Fracture Toughness Determinations by Indentation, A. G. Evans and E. A. Charles, J. Amer. Ceramic Soc. 59, July-August 1976, p. 371-372.

of radius from ~50-200 μm . In relatively fine uniform materials the reproducibility is relatively good. At a load of 2 Kg the reproducibility in 2a was ~1.5% for 10 tests, while the reproducibility in 2c was about 6%. However, several of the materials tested had less uniform microstructures and there was a corresponding decrease in the 2a and 2c reproducibility to ~3% and 18% respectively. The reproducibility should therefore be a very useful parameter in ranking the microstructural uniformity of materials.

The crack patterns observed generally approximated the ideal half penny median cracks expected⁴. There was evidence of lateral cracking during unloading particularly at loads greater than 2 Kg. Many times this lateral cracking with a spallation did not occur for several hours after unloading. However, this lateral cracking is not of direct concern in the analysis and in the limited cases studied there was no noticeable effect of time on the median crack formation. The tendency for non-ideal⁸ crack patterns increased with load above 5 Kg, especially for the coarser materials (e.g., 330-64, Fig. 8) . This observation has made it very difficult to obtain good data at the large values of load and c/a required by the analysis⁴ for the

⁴Fracture Toughness Determinations by Indentation, A. G. Evans and E. A. Charles, J. Amer. Ceramic Soc. 59, July-August 1976, p. 371-372.

⁸A critical Evaluation of Indentation Techniques for Measuring Fracture Toughness: I. Direct Crack Measurements, G. Antis, P. Chantikul, R. Lawn, D. Marshall, J. Amer. Ceram. Soc. 64, Sept. 1981, p. 533.

determination of K_{IC} . Fortunately, the data for smaller loads can be analyzed in the spirit of Ref. 4 to yield very good results.

Equation 8 of Ref. 4 can be rearranged to yield,

$$a^2 = \frac{\phi}{.15k} \frac{K_{IC}}{H} c^{3/2} \quad c \gg a \quad (1)$$

where K_{IC} is the critical stress intensity factor, H is the high load hardness, ϕ is a constraint factor ~3 and k is a free surface correction evaluated from experimental data. The value of k was found⁴ to be about 3.2. Values of K_{IC} were determined for nine silicon carbide materials using the above equation with values of c/a to about 4. There was a pronounced c/a dependency for the calculated value of K_{IC} , with a steadily falling value as c/a increased, even for a range of c/a where the data of Ref. 5 indicated the contrary.

If it is assumed that K_{IC} and H are indeed material properties and remain constant throughout the load range of crack propagation and in addition that the differential form of Eq. 1 describes the change in crack length (dc) with change in impression da . Then cracking occurs at constant K_I and

$$2ada = \frac{\phi}{.15k} \frac{K_{IC}}{H} \frac{3}{2} c^{1/2} dc \quad (2)$$

and an integration of Eq. 2 yields;

⁴Fracture Toughness Determinations by Indentation, A. G. Evans and E. A. Charles, J. Amer. Ceramic Soc. 59, July-August 1976, p. 371-372.

$$a^2 = \frac{\phi}{.15k} \frac{K_{IC}}{H} c^{3/2} + I \quad (3)$$

Equation 3 can be tested for validity over a wide load range. The integration constant I can most appropriately be evaluated for the condition where a propagating crack first appears, i.e., where $c = c^* = a^*$ for a load P^* .

Data for nine materials were least square fitted to Eq. 3 over loads ranging from 1/2 to 5 Kg and corresponding large variations in a and c , with c/a down to 1.5. Data fits to other powers for c and a as well as for exponential and log curves were also tried. Fits stemming from more elaborate forms of Eq. 1 which account for elastic corrections^{4,8} by introducing the ratio of hardness to elastic modulus were not successful. Moreover, these corrections should be relatively minor in comparing materials with relatively little variation in these parameters. The data were fit very well by Eq. 3 and in all cases gave higher coefficients of determination than any other fits tried. The constants in equations of the form:

$$a^2 = Bc^{3/2} + A \quad (4)$$

⁴Fracture Toughness Determinations by Indentation, A. G. Evans and E. A. Charles, J. Amer. Ceramic Soc. 59, July-August 1976, p. 371-372.

⁸A critical Evaluation of Indentation Techniques for Measuring Fracture Toughness: I. Direct Crack Measurements, G. An. S., P. Chantikul, R. Lawn, D. Marshall, J. Amer. Ceram. Soc. 64, Sept. 1981, p. 533.

are given in Table II. The coefficients of determination indicate excellent fits even for several materials with limited data (329-71, 330-38) and with highly variable structures (NC433). The experimental values of B and A allow the direct determination of a^* or c^* , as well as K_{IC}/H which has special significance as a brittleness measure⁶.

In order to obtain K_{IC}/H and subsequently K_{IC} , a value for the constant ϕ/k must be obtained. This is most appropriately done for a material of known properties such as NC203. Although there is some disagreement on the K_{IC} of NC203 (hot pressed SiC) the value adopted is that of Ref. 4, namely $K_{IC} = 4.00 \text{ MPa}\cdot\text{m}^{1/2}$. The hardness used, $H_V 2100 \text{ Kg/mm}^2$ was that found in this study by the method described subsequently. Using the experimental B and H_V for NC203 and the presumed value of K_{IC} the constant $\phi/k = .7163$, which agrees well with that suggested⁴ , $\phi/k = .9375$.

As more data is added B may shift slightly and K_{IC} for the actual material at hand may prove to be different from 4.00 $\text{MPa}\cdot\text{m}^{1/2}$. In any case, one material with independently measured K_{IC} , together with the load variation of 2a and 2c fixes all the disposable constants.

⁴Fracture Toughness Determinations by Indentation, A. G. Evans and E. A. Charles, J. Amer. Ceramic Soc. 59, July-August 1976, p. 371-372.

⁶Hardness, Toughness and Brittleness: An Indentation Analysis, B. Lawn and D. B. Marshall, J. Amer. Ceramic Soc. 62, August 1979, p. 347-350.

TABLE II. SUMMARY OF INDENTATION DATA FITS

MATERIAL	SLOPE B (mm ² •10 ⁻²) ^{1/2}	CONST. A (mm ² •10 ⁻²) ²	COEF. OF DETERMIN. r ²	GR(PTS); LOADS N(n);KG	SLOPE B' KG/(mm ² •10 ⁻²) ²	CONST. A' KG	COEF. OF DETERMIN. r ²	GR(PTS); LOADS N(n);KG
NC203(1)	.2929	.4684	.9998	3(16);1,3,5	.4530	.2433	.9985	3(16);1,3,5
α -SiC(78)(1)	.2665	.3170	.9969	3(15);1,2,5	.4750	.2160	.9997	3(15);1,2,5
NC433(1)	.3654	.0671	.9890	3(15);1,2,3	.3769	.2824	.9939	3(15);1,2,3
329-53	.2065	.9351	.9961	4(20);1,2,5	.4231	.1716	.9997	4(20);1,2,5
329-71	.3180	.9460	.9420	1(9);1,2,5	.4477	.0728	.9999	3(9);1,2,5
330-12	.2883	.3366	.9928	4(12);1,2,5	.4081	.0587	.9999	3(10);1,2,5
330-38	.3698	.0411	.9988	1(8);1/2,1,2	.4043	.0335	.9995	3(10);1/2,1,2
331-2B	.2573	.5844	.9950	3(20);2,3,5	.4422	.0623	.9995	3(20);2,3,5
331-31E	.3049	1.0781	.9972	3(20);1,2,5	.4050	.0608	.9998	3(20);1,2,5

Samples studied in AMMRC TR-80-15; Ref. (1).

For the choices at hand,

$$K_{IC} = 6.503 \cdot 10^{-3} H_V B \quad \text{MPa} \cdot \text{m}^{1/2} \quad (5)$$

where H_V is Kg/mm^2 and B is $(\text{mm} \cdot 10^{-2})^{1/2}$.

The value of a^* or c^* is obtained from the solution of

$$a^{*2} - B a^{*3/2} - A = 0 \quad (6)$$

Values of a^* are given in Table III.

The value of hardness called for in Eq. 3 should also be constant in the crack propagation range. If so, P should be related to a^2 as

$$P = \frac{H_V}{\alpha} a^2 + I = B' a^2 + A' \quad a > \frac{I}{B'} \quad (7)$$

Where $\alpha = .4636$ for the Vickers geometry, P is load in Kg , and $I = 0$ only if the hardness is independent of P for all a . Such is usually not the case for very hard materials at low loads ($< 1\text{Kg}$) and small a . Experimental fits for the constants A' and B' show the expected good correlation to a^2 dependency, but with $I \neq 0$. The results are given in Table II. The values adopted for H_V are evaluated from B' as,

$$H_{V\infty} = 4636 B' \quad \text{Kg}/\text{mm}^2 \quad (8)$$

where B' is $\text{Kg}/(\text{mm} \cdot 10^{-2})^2$. $H_{V\infty}$ corresponds to the H_V that would be obtained at large loads where $A' \ll B' a^2$. The value of P for a^* may be calculated from Eq. 7 and corresponds to the maximum load that can be sustained without formation of a crack while c^*

TABLE III. CALCULATED RESULTS

MATERIAL	C [*] μm	P [†] KG	H _{V00} KG/mm ²	K _{IC} •m ^{1/2} MPa	Si Vol.%	Grains/Si μm/μm	4 PT.	
							CHAR. STR. MPa	K _{IC} /H (μm) ^{1/2}
NC203(1)	8.31	.556	2100	4.00(2)	0		610,712(3)	.194
α-SiC(78)(1)	6.84	.438	2202	3.82	0	8,2(7)	384	.176
NC433(1)	3.99	.342	1747	4.15	13-25(1)	7,3(8)	350	.242
329-53	10.80	.665	1961	2.63	10(4)	<1,1.15		.137
329-71	11.59	.674	2076	4.29	8(4)	7,2		.211
330-12	6.82	.248	1892	3.55	12(6)-23	7,3	530,164(9)	.191
330-38	3.37	.080	1874	4.51	12(4)	5,4	225(5),109(9)	.245
331-2B	8.96	.417	2050	3.43	10(6)-13(4)	9,3	660	.170
331-31E	12.2	.664	1878	3.72	15(6)-18(4)	1.5,1		.202

¹Samples studied in AMMRC TR-80-15; Ref. (1).²Constants set so K_{IC} = 4.00 MPa•m^{1/2}; Ref. (4).³Poor fit-avg. str. 582 MPa, 683 MPa.⁴Calculated from skeleton density.⁵Extensive machining damage.⁶X-ray analysis.⁷Pores up to 20 μm; Ref. (1).⁸Si lakes >100 μm; Ref. (1).⁹Unmachined.

or a^* are the maximum dimension of indentation damage that can be tolerated without a crack developing. The significance of similar parameters is discussed in Ref. 6.

Equation 7 may be tested in another way since, $A' \neq 0$ there should be a smooth variation with the load P of the H_V calculated in the usual way. The usual calculation of hardness is

$$H_V(\text{calc}) = \frac{\alpha P}{a^2} \quad (9)$$

Equation 9 may very well fit the facts for $a < a^*$ but certainly does not for $a > a^*$ as shown in Table II. If Eq. 7 is substituted in Eq. 9,

$$H_V(\text{calc}) = \alpha B' \left[1 + \frac{A'}{(P-A')} \right] = H_{V\infty} \left[1 + \frac{A'}{(P-A')} \right] \quad (10)$$

It is easily seen that the load dependency of $H_V(\text{calc})$ is small if A' is small or if $P^* \gg A'$. However, for low loads the second term in Eq. 10 may be very large. Table IV shows the average experimental values of the hardness determined from Eq. 9, $H_V(\text{obs})$, together with those calculated from Eq. 10, $H_V(\text{calc})$ and the value H_V^* , at P^* . The calculated values agree within the standard deviation of the measurement. The values H_V^* for $\alpha\text{-SiC}(78)$ and NC433 are undoubtedly too high. They will be unduly subject to error, particularly from the fit which determines a^* , which is relatively poor for these materials. However, it is easily understandable that values of "microhardness" for SiC are often reported above 3000 Kg/mm^2 . It is also clear that the analysis gives a good explanation for

TABLE IV. EFFECT OF LOAD ON OBSERVED VICKERS HARDNESS.

MATERIAL	LOAD Kg	H_V (Obs.) Kg/mm ²	PTS. n	STD. Kg/mm ²	DEV. Kg/mm ²	H_V (Calc.) Kg/mm ²	H_V^{*} Kg/mm ²	H_V^{∞} Kg/mm ²	a^* μm	P^* Kg
NC203(1)	1	2890	6	256	22	2775	3734	2100	8.31	.556
	3	2218	5	15	2285	2207				
	5	2230	5							
α-SiC(78)(1)	1	2940	5	35	53	2808	4344	2202	6.84	.438
	2	2415	5	59	2468	2302				
	5	2316	5							
NC433(1)	1	2594	6	266	2434	(10026)	1747	3.99	.342	
	2	1941	5	92	2035					
	3	1971	4	82	1929					
329-53	4	2265	4	65	2368	2644	1961	10.80	.665	
	2	2172	13	26	2146					
	5	2030	3	25	2031					
329-71	1	2240	3	112	2239	2327	2076	11.60	.674	
	2	2175	3	250	2154					
	5	2110	3	100	2106					
330-12	1	2022	5	93	2010	2479	1892	6.82	.248	
	2	1945	5	37	1949					
	5	1915	5	24	1914					
330-38	1/2	1954	5	64	2008	3225	1874	3.37	.080	
	1	1984	5	68	1939					
	2	1898	5	31	1906					
331-2B	2	2142	10	61	2116	2410	2050	8.96	.417	
	3	2082	5	35	2093					
	5	2070	5	69	2076					
331-31E	1	2020	4	65	2000	2069	1878	12.20	.664	
	2	1923	14	50	1936					
	5	1905	2	35	1901					

the high apparent hardness shown by these materials at loads as high as 1-2 KG.

The results of the indentation analysis are yet too few to draw any conclusions. However, the following points are clear. First the use of H_{V0} appears to have significant merit since it eliminates the rather wide apparent hardness variations that some materials show at low loads. Also the use of fitted data gives a load independent K_{IC} of approximately the expected value.

The data for volume %Si and grain size estimates in Table III are not yet refined enough to allow firm conclusions on the effect of Si content and grain size on hardness or K_{IC} . The results for K_{IC} are in the range expected but, surprisingly, several materials show K_{IC} higher than for NC203. These variations may yet prove to be within the reproducibility range of the method. The K_{IC} for the very fine grained sample (329-53) was abnormally low (2.63 MPa-m^{1/2}). This could be a valid effect of silicon lake size or may reflect very high residual stress in this sample. The sample was a shell ~3 mm thick surrounding a central section of unreacted carbon ~2 mm thick. The reacted shell would be stressed in tension during cooling by the carbon core and may have contributed to the lower than expected fracture toughness.

The values for c^* and p^* show more difference between materials than either K_{IC} or H_{V0} . High values for both c^* and p^* should be helpful in engineering applications since such materials should tolerate surface loading better.

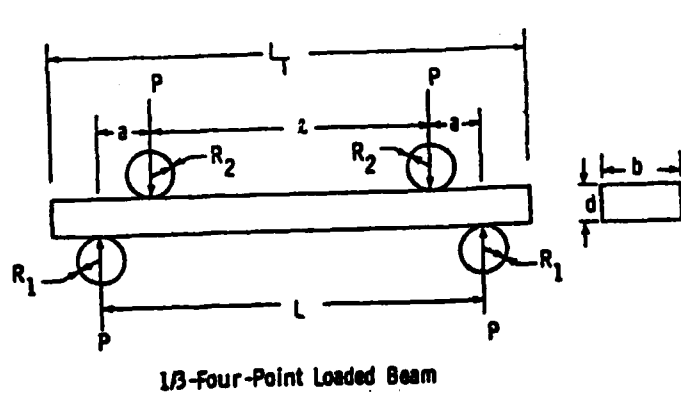
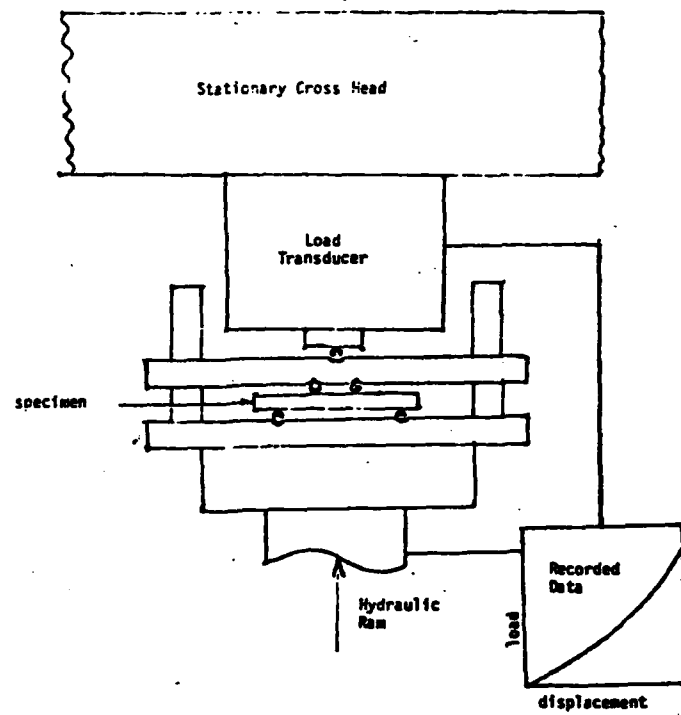
The data fits for P vs. a^2 and a^2 vs. $c^{3/2}$ guarantee that K_{IC} and H_V will be independent of load. Only the quality of fit and correspondence to independently measured values of K_{IC} can test the correctness of this view.

Strength Testing

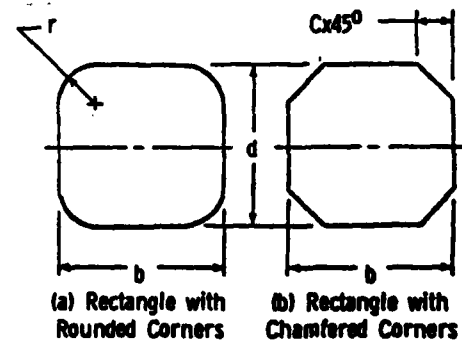
Flexure strength was determined for each lot of material by slowly stressing to fracture in four-point bending small rods of rectangular cross-section. The specimens had a nominal volume and surface area of $1.6 \cdot 10^{-7} \text{m}^3$ and $3 \cdot 10^{-4} \text{m}^2$, respectively. An MTS Series 810 servohydraulic test system was equipped with a four-point bend fixture and tests were conducted under displacement control at a constant displacement rate of $4.2 \times 10^{-3} \text{ mm/sec}$. The test fixture was attached to the hydraulic ram and during testing the ram and fixture were brought into contact with a knife edge which was rigidly attached to a load transducer. During testing, analog signals for load and displacement were recorded with an x-y recorder. The load at fracture was used to compute the flexure strength.

The specimen and testing configurations are shown in Fig. 10. The test fixture is a standard 1/3-four-point bending configuration. However, errors due to nonstandard specimen configurations and other errors were considered in the final analysis of the data. In assessing testing errors, the procedures currently under study at AMMRC were followed. The

*to be published.



1/3-Four-Point Loaded Beam



Beam Cross Section

Figure 10. Strength Testing Fixture and Sample Geometry.

following were the estimated errors in measurement of flexure strength determined from tables of errors supplied by AMMRC.

<u>Source of Error</u>	<u>Computation</u>	<u>Error Est. (%)</u>
Simple beam assumptions		
- linear stress distribution	$a/d = 5.1$	-0.3
- initial beam curvature	$R_c/d > 100$	$<-0.3 \approx 0$
- anticlastic curvature	$\frac{b}{d} = \frac{.104}{.375} = .28$	0
- large deflection	$\frac{2a}{d} = 10.1$	+0.1%
Error due to specimen chamber		<u>+3.25%</u>
Total error		<2.75%

The errors due to external influences arising from fixture misalignment, friction, specimen twisting and other sources have not yet been fully analyzed. The sources of error are being studied and future data will be corrected accordingly. The data thus far were obtained with force measurement on the lowest scale of a 10,000 lbf transducer which gives poor sensitivity at small breaking loads. Calibration of this lowest scale with a proving ring gave good results and a limited number of confirming tests were carried out on an Instron equipped with a far more appropriate load transducer. However, an improvement in the accuracy of load and displacement measurement will be achieved by the installation of a new 1000 lbf load transducer and the use of a more sensitive displacement transducer which will be attached near the specimen loading points.

A self-aligning flexible fixture similar to that described⁹ is planned. This fixture in testing graphite consistently gave results ~30% lower than fixtures with fixed pivot points. Such large effects are not expected with SiC since the elastic deflections are much smaller, but nonetheless this source of error bears investigation.

Most samples were ground with the procedure specified in Ref. 1 with finishing scratches (600 grit) parallel to the bar length. Two different shops performed the finishing and a low magnification inspection showed many bars with visable defects (cracks) and chips at the chamfered corners. A cursory consideration of surface finishing suggests that it is relatively easy to provide a smooth enough surface to avoid scratches that would be strength limiting. For example, typical finish grinding would leave scratches less than 1 μm deep. Such smooth surfaces are, however, not sufficient if rough grinding has introduced subsurface damage areas of the size range of 50 μm . A systematic study of machining damage in silicon carbide has been published¹⁰. Two lots (330-12 and 330-38) were tested at AMMRC with no finishing except the hand grinding of several silicon beads from the surface so that good contact could be made in the

⁹Test Geometry and Its Effect on Graphite Flexural Strength in Four Point Bending, E. Morris, S. Lewallen; Extended Abstracts, 15th Carbon Conference, Philadelphia, PA, June 1981, American Carbon Society.

¹⁰Surface Finish Effects and the Strength-Grain Size Relation in SiC, Cranmer, Tressler and Bradt, J. Amer. Ceram. Soc. 60, May-June 1977, p. 230-232.

loading fixture. Other samples of the same 330-12 lot were also finish ground for comparison.

The fractured bars were inspected with a binocular microscope and in some cases with SEM for obvious flaws, but no attempt was made to carry out a detailed failure analysis.

The results for the materials tested together with some comparison tests from Ref. 1 are presented in Table V with Weibull plots in Figures 11-18. The Weibull characteristic strength, η , is the stress required to give a cumulative failure probability of 63.2%. Due to the small number of samples, (N_0), the evolution of specimen preparation, and testing technique, the results must be viewed as preliminary. Several rather obvious results are apparent.

First the strength of very coarse structures is low. The bars of 330-64, while made from a very fine skeleton, were known to have a structure similar to that of Fig. 8. The Weibull characteristic strength, 190 MPa, is the lowest of any of the ground materials examined. The fit to a Weibull distribution (Fig. 18) is not good which may reflect the small number of samples but more probably the existence of a population of machining flaws. Such a coarse structure would be expected to show severe damage with single grain fractures.

It is also quite obvious that the "unmachined" bars were vastly inferior to their ground counterparts (330-12). However, in this case the difference is probably due to two factors. The first is the obvious effect of finish machining versus an as

TABLE V. SUMMARY OF STRENGTH PROPERTIES

MATERIAL	TESTS n	HIGH		LOW		WEIBULL MODULUS	STD. MPA	DEV. MPA	WEIBULL		STRENGTH CONTROL
		MPa	MPa	MPa	MPa				CHAR. MPa	STR. MPa	
NC203 (1)	127	825	477	683	10 (2)	65	610	712 (2)	Machining	Defects	
α -SiC(78) (1)	36	449	224	363	10.6	45	384		Large grains; Large Agglom.; Pores		
NC433 (1)	37	383	169	317	14.9 (2)	65	350 (2)		Large grains; Large Si lakes		
330-12 Unmachined-AMMRC	16	300	28	164	(1.69) (3)	78	(164) (3)		Surface damage; Grain growth zone		
Ground	18	690	281	459	(4.54) (3)	105	(530)		Unknown		
330-38 Unmachined-AMMRC	16	170	30	109	(2.23) (3)	39	(109) (3)		Surface damage; Grain growth zone		
Unmachined-U of M	8	295	172	224	(3.54) (3)	45	(225) (3)		Surface damage; Grain growth zone		
330-64 Ground	9	259	181	139	(4.38) (3)	46	(190) (3)		Very large grains		
331-2B Ground	12	855	351	593	(4.16) (3)	161	(660) (3)		Unknown		

TEST CONDITIONS: One third-4 point bending; Displacement Rate $4.2 \cdot 10^{-3}$ mm/sec.
 Spans - .95 cm; Nominal Stressed Volume $1.6 \cdot 10^{-7}$;
 Nominal Surface $3 \cdot 10^{-4}$ m²; Ground Samples 600 Grit finish.

¹Samples and Results, Ref. (1).

²Poor Fit.

³Very poor fit to Weibull distribution.

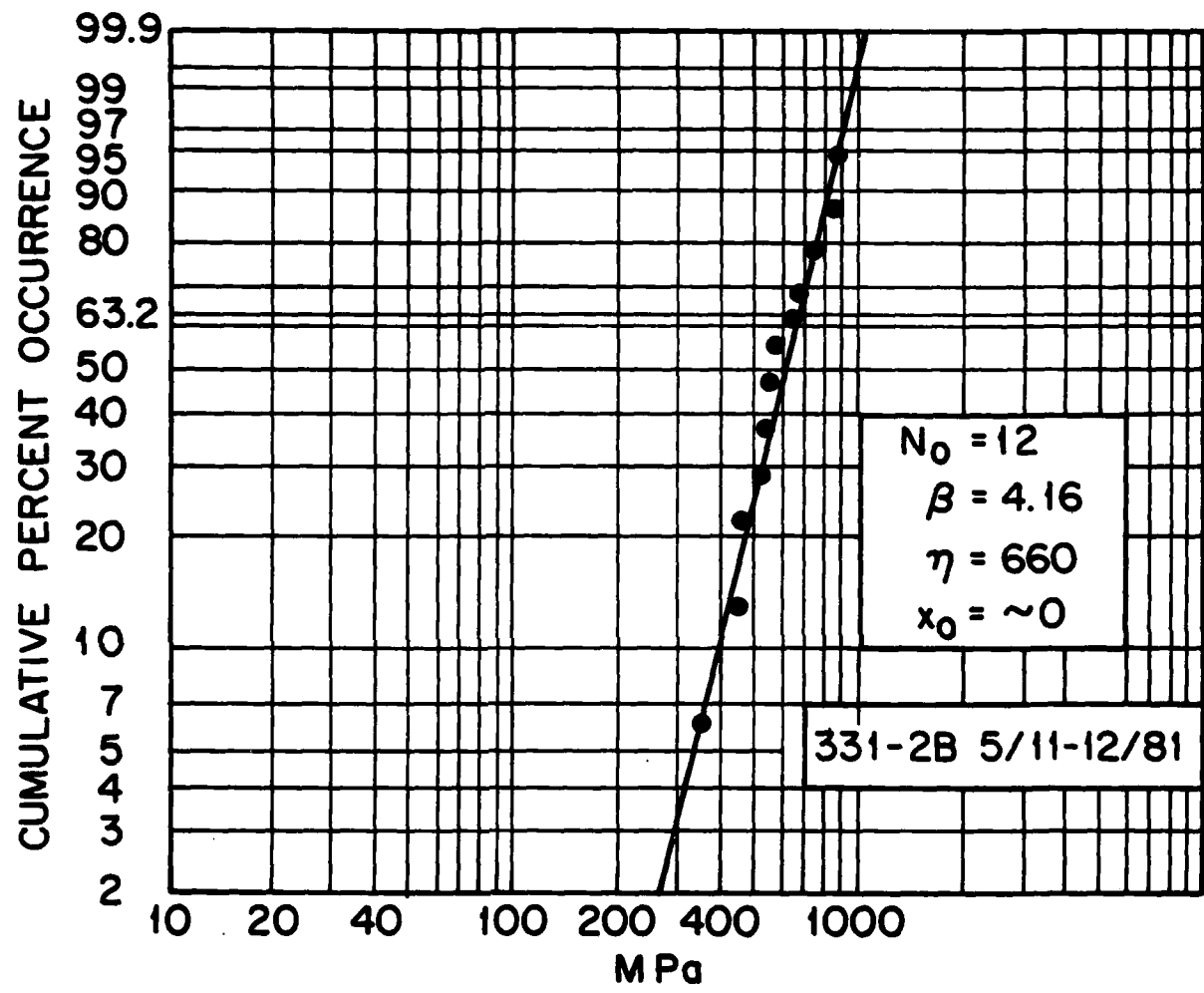


FIGURE 11.

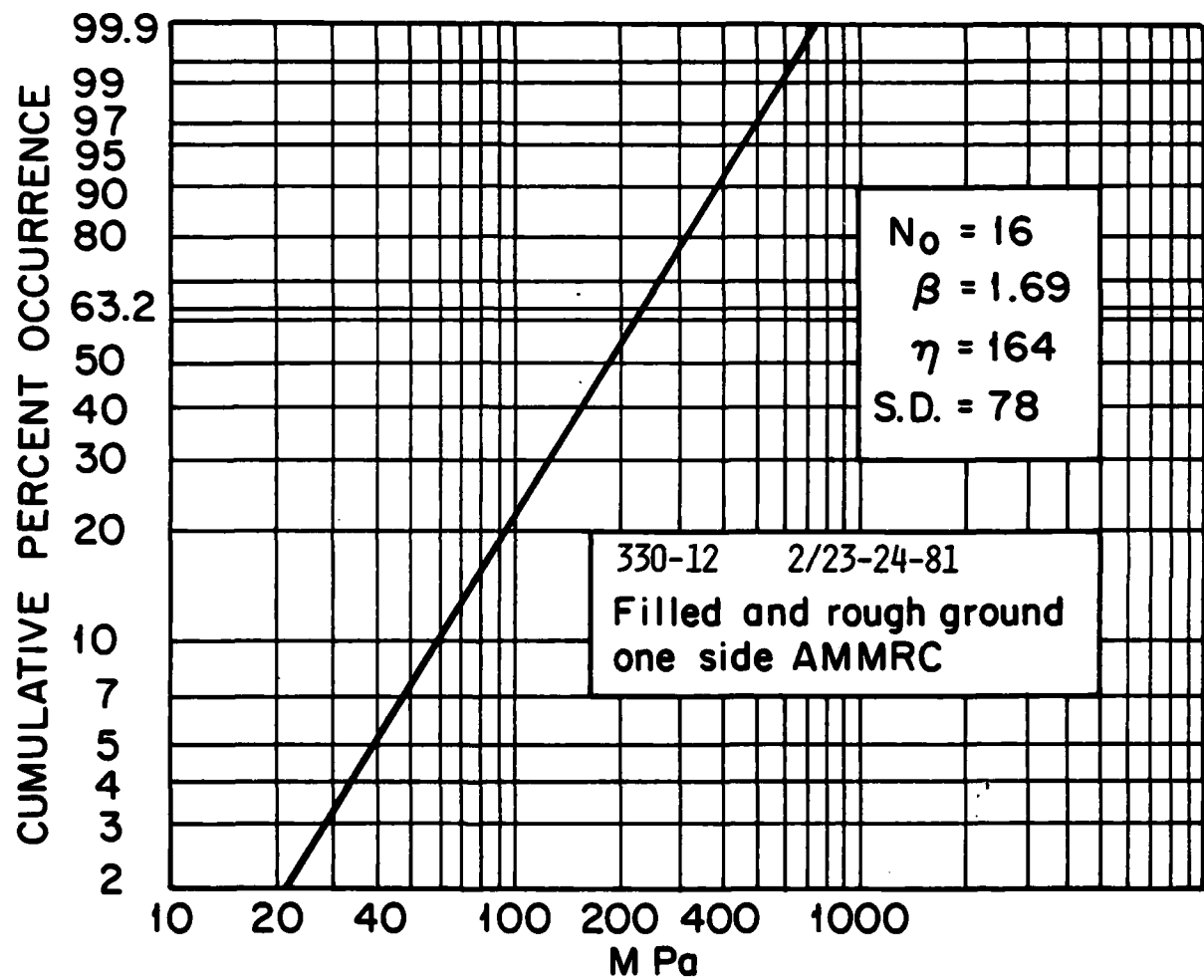


FIGURE 12.

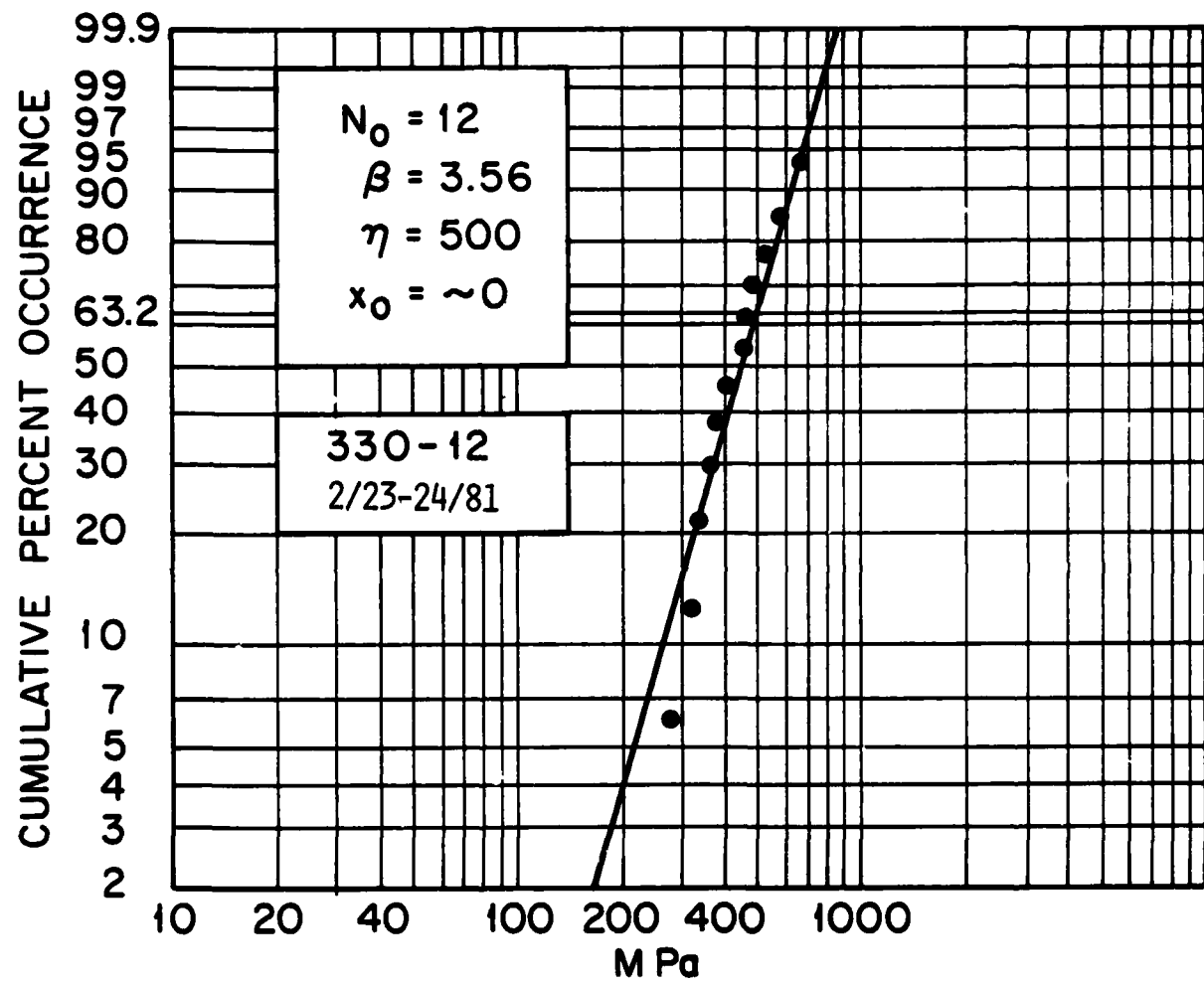


FIGURE 13.

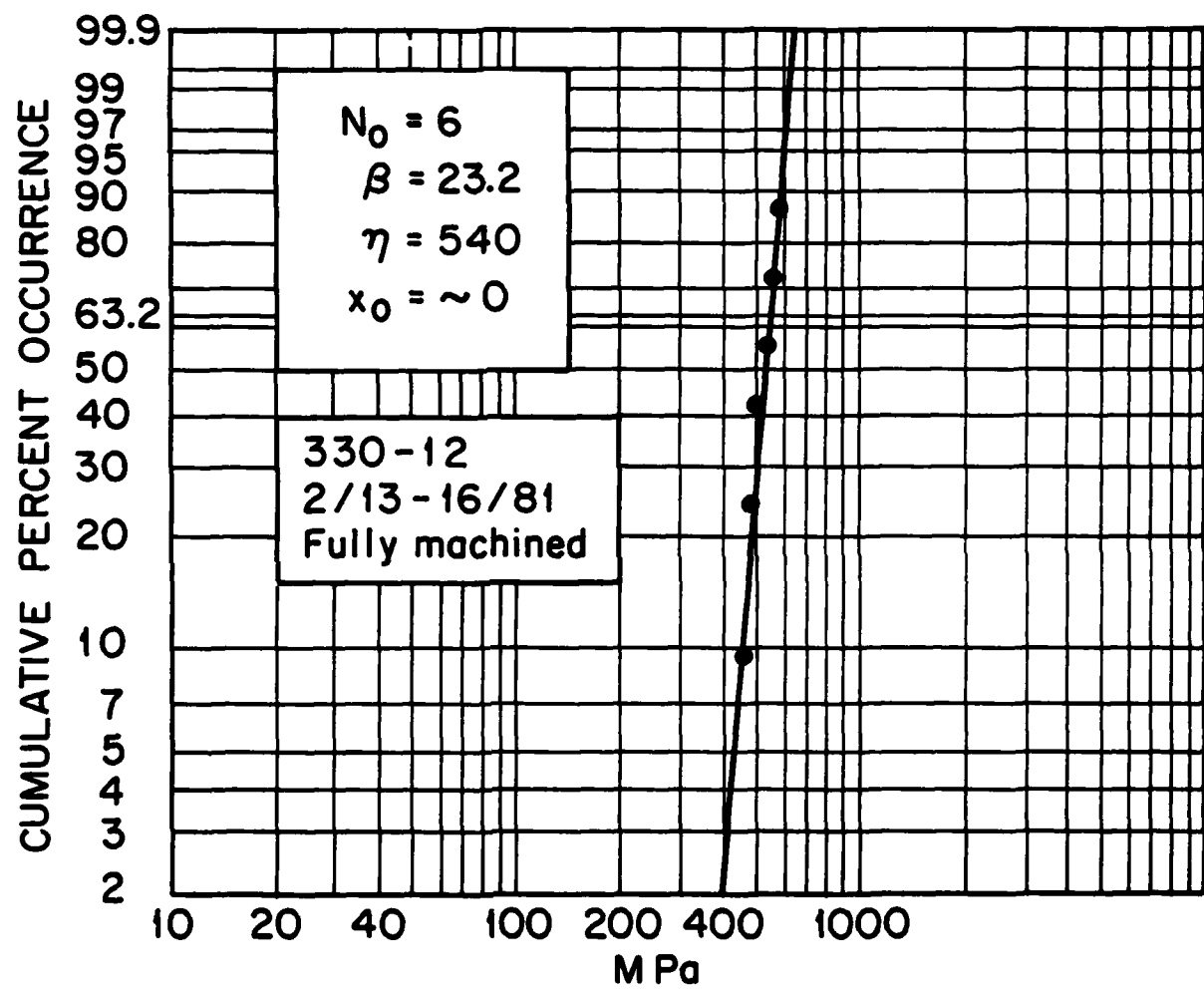


FIGURE 14.

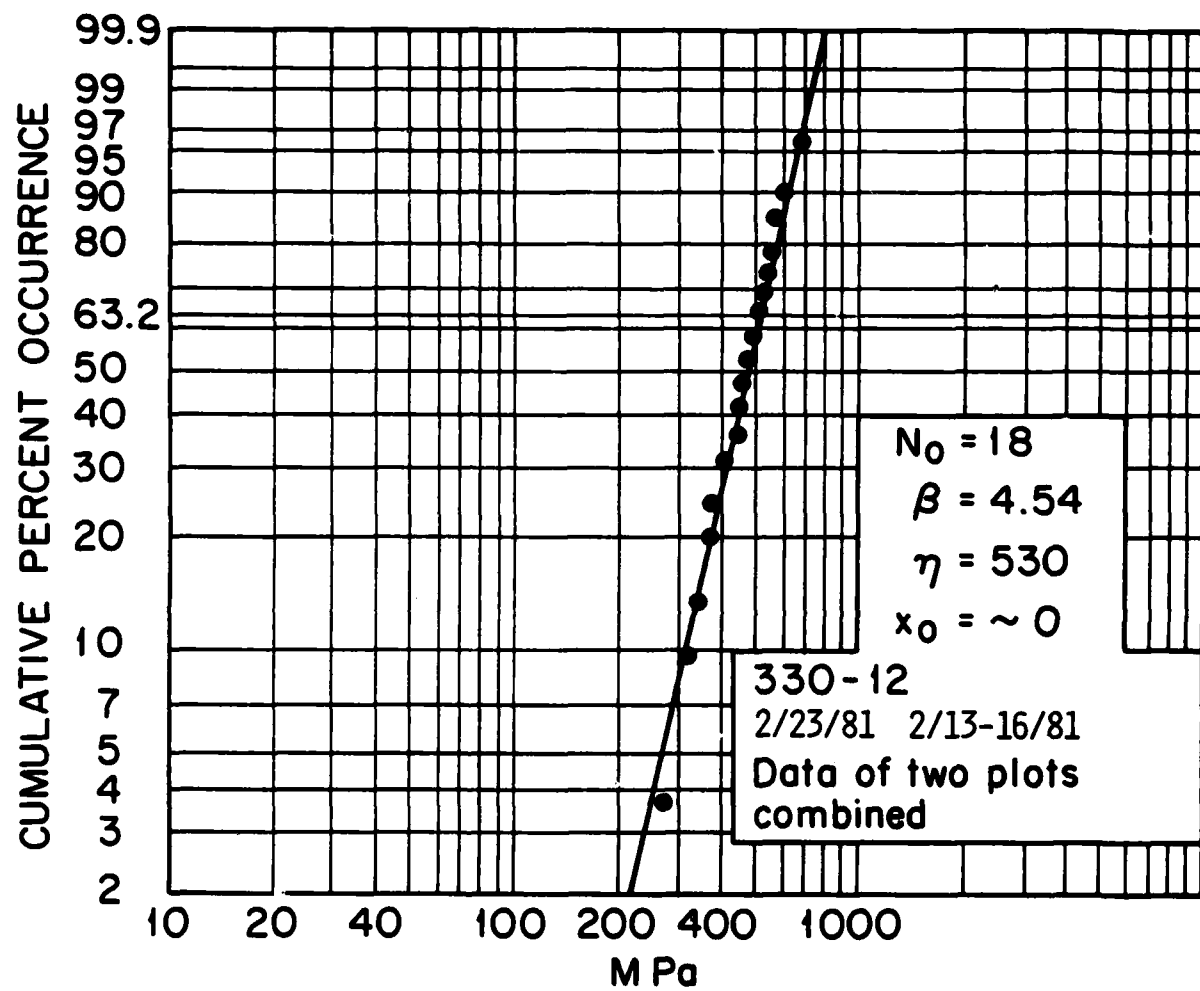


FIGURE 15.

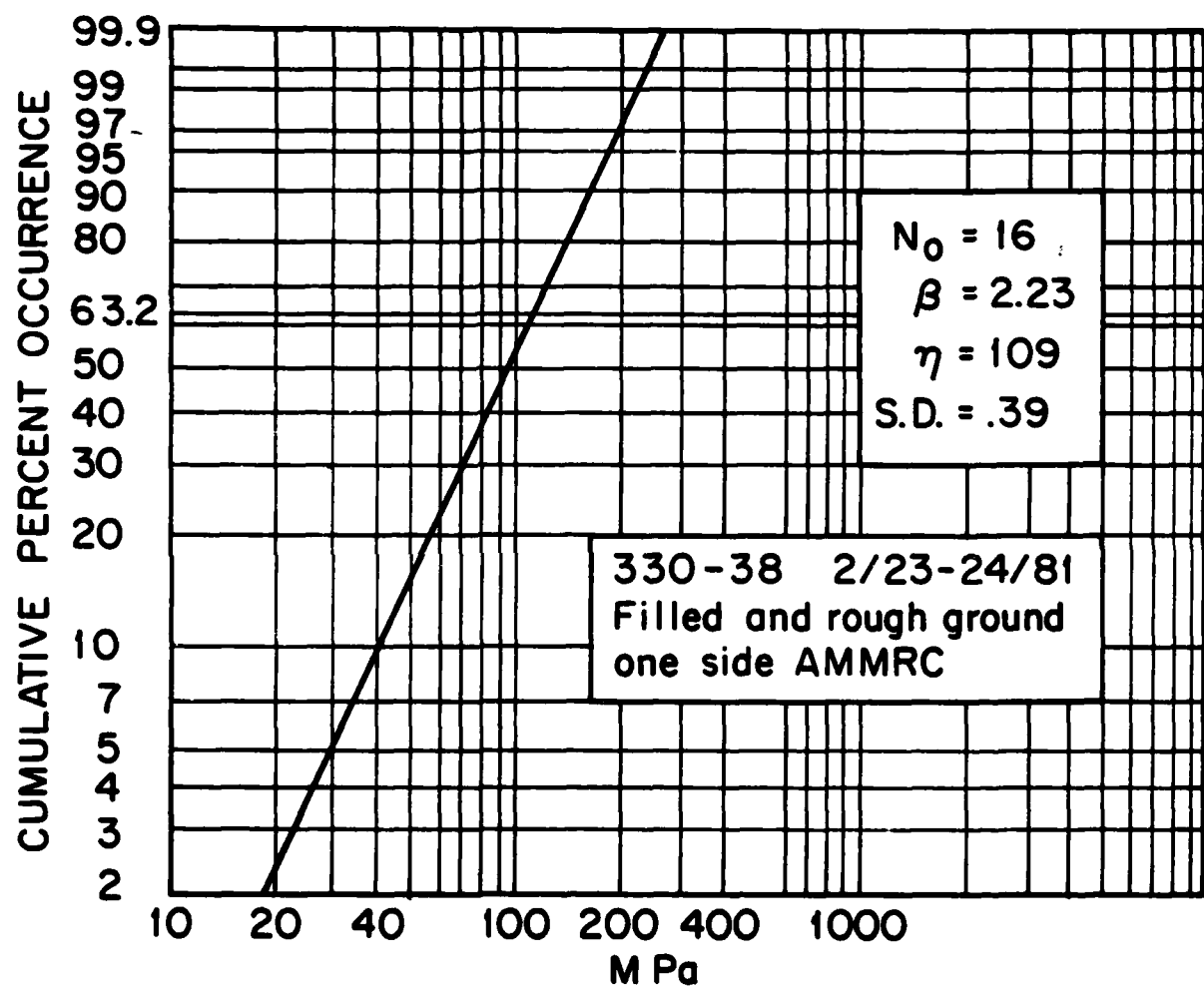


FIGURE 16.

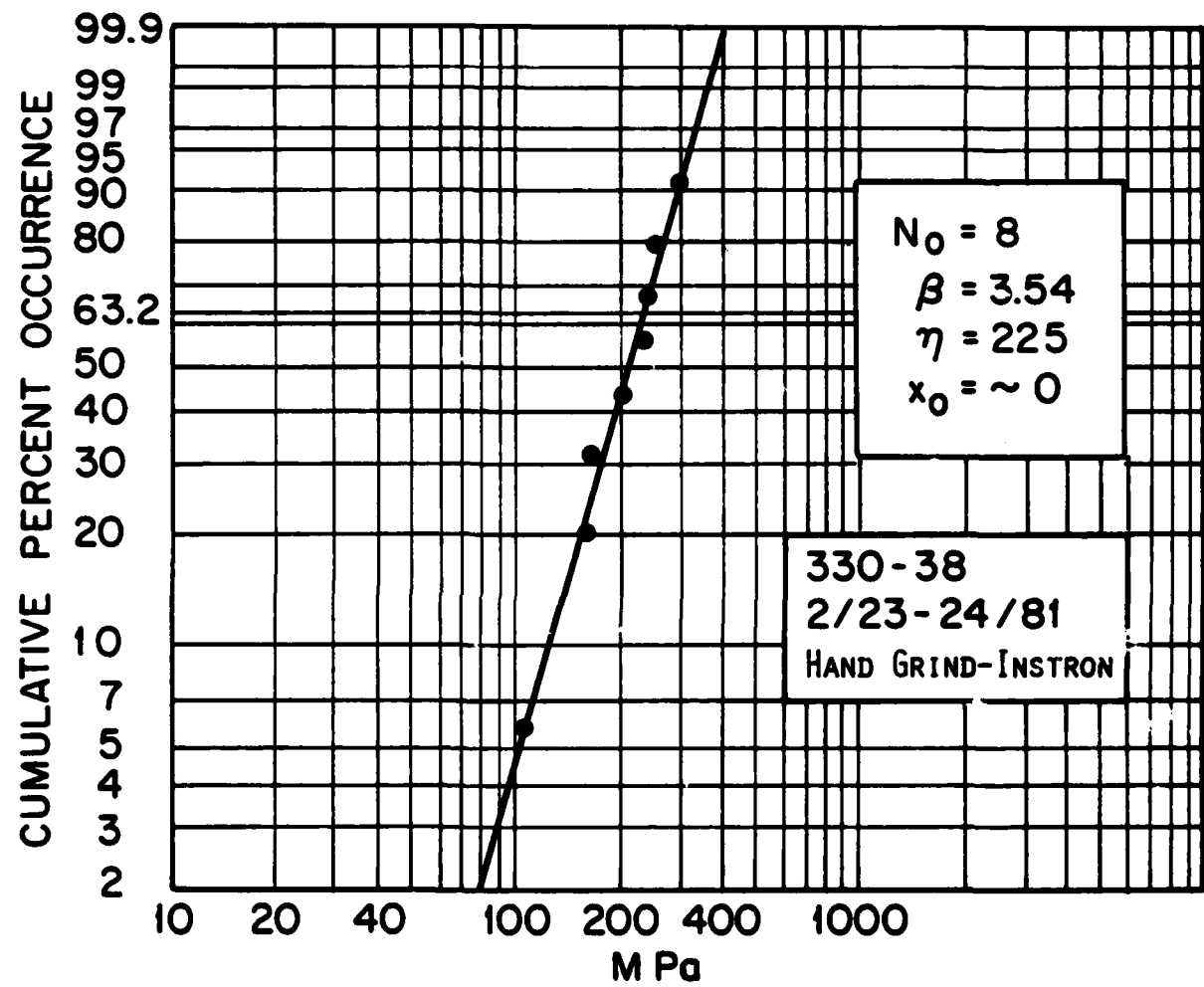


FIGURE 17.

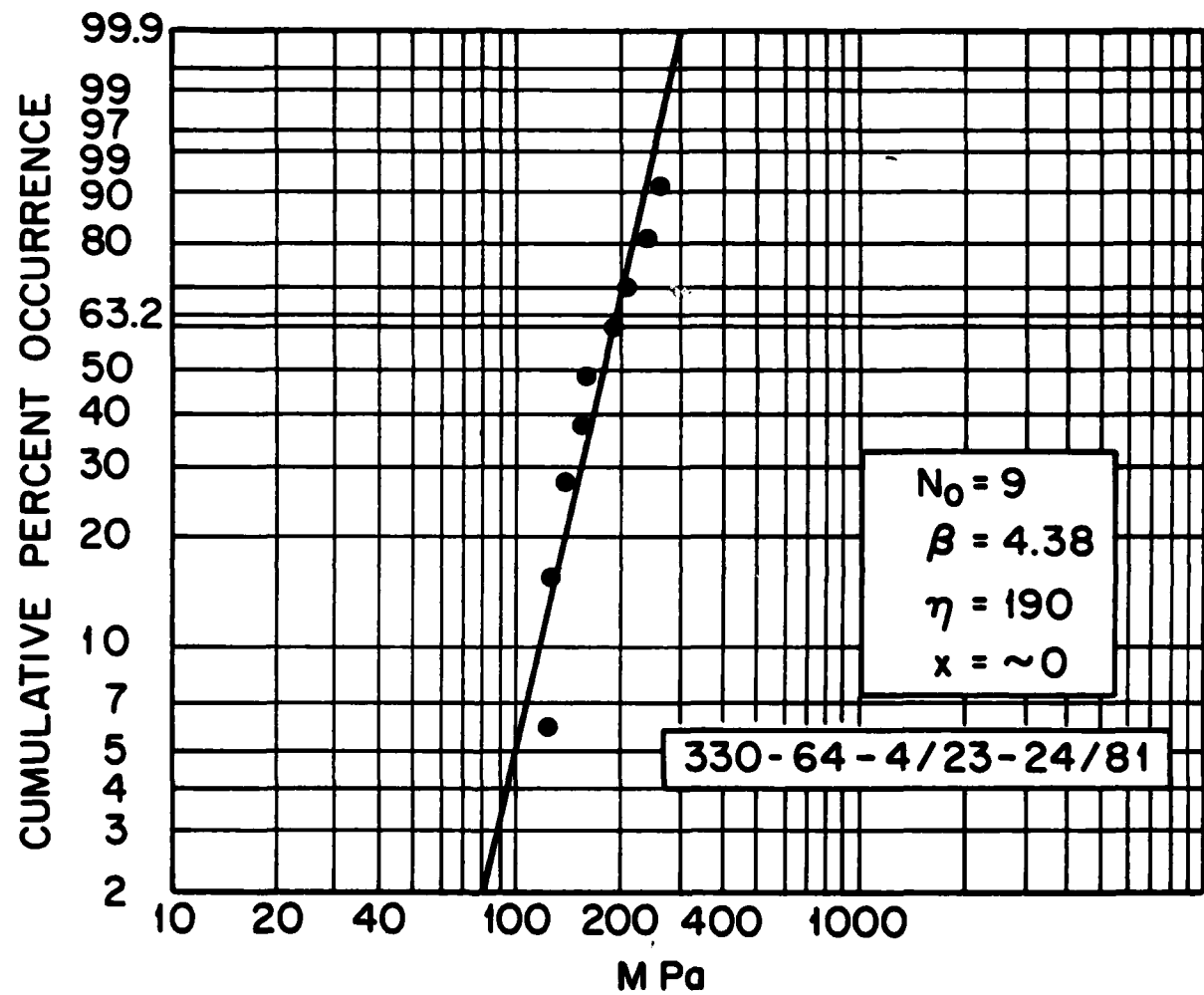


FIGURE 18.

processed surface which includes the potential damage from chipping as silicon beads were removed. However, of more importance is that in the particular samples there was an extremely coarse reaction zone just under a fine grained surface. The reaction zone was at least partially removed during the finishing. However, failure to completely remove the zone would make matters worse since it would now be at the stressed surface. None of the sample lots fits well to a Weibull distribution with the exception of the very small lot (6 bars) of 330-12 (Fig. 14) processed separately from the rest. This good fit and abnormally high Weibull modulus, $\beta = 23$, is probably due to the small number of samples. The combined lots (18 tests) of machined 330-12 (Fig. 15) show a very respectable strength level. The characteristic strength of 530 MPa exceeds any of those studied in Ref. 1 except hot pressed SiC (NC203). It exceeds α -SiC(78) (sintered) in all respects except in Weibull modulus, which may be caused by a machining defect flaw population. The structure of 330-12 is shown in the top row of Fig. 9.

The properties of 331-2B (Fig. 11) are extremely encouraging even though only a small number of tests (12) has been completed. The structure of this material is that of the second row from the top in Fig. 9. This material compares favorably with hot pressed SiC (NC203) and far exceeds all others which include various reaction bonded and sintered materials. The highest strength exceeds any found in 127 tests of NC203 and its characteristic strength, 660 MPa, exceeds that (610 MPa) of the

largest group of NC203 samples tested in Ref. 1. The Weibull modulus is relatively low (4.16) which may be due to inadequate sample or a dual flaw population from machining.

At this stage there is inadequate data to draw any firm conclusion about the strength relation to microstructure. However, the trend is hopeful since the strengths of 330-12 and 331-2B are progressively higher as the structure is refined. These materials represent the first two steps down the middle column of Fig. 9.

CONTINUING WORK

Carbon Skeleton

The next adjustments of the carbon skeleton will involve further optimizations of the pore size-particle size changes already begun. In addition several carbons with small controlled variations in density in the range $.85 \text{ gm/cm}^3$ to $.90 \text{ gm/cm}^3$ will be produced in both "fine" and "coarse" skeletons. These should allow a systematic comparison of the effect of volume % Si on the final properties.

Substantial variation in the polymer curing time and temperature will be investigated in order to further improve the shape stability of thin pieces machined from the polymer.

Siliconization

With the availability of skeletons with slight density variations an effort will be made to delineate the region of fluid flow control. Some limits on reaction depth versus time at various pore sizes and total pore volume will be sought.

In addition post heat treatment of siliconized samples to obtain controlled coarsening of the structure will be attempted. In principle such a treatment could affect the whole sample and not just small regions of a sample as is now the case when the coarsening results from uncontrolled reaction exotherms.

Property Evaluation

Indentation analysis will be extended to additional samples and will include additional data to existing samples so that the overall usefulness of the method can be appraised. Independent measurement of K_{IC} will be made on several materials to act as a check on the indentation method.

Additional fixture modifications, a new load cell, refinements in test procedures and data reductions will be made for the four point bend testing. These changes should greatly improve confidence in the results. In addition a bi-axial loading test employing a punch loading of a 3 point supported disk¹¹ is to be made on several materials. This test has shown very reproducible results on other ceramic materials, allows some advantages in sample preparation, and gives a means of testing a relatively large stressed volume. The test fixture has been obtained and samples are in final stages of preparation.

In addition, more tests are planned with unmachined surfaces and with surfaces that have been etched.

¹¹Biaxial Flexure Strength of Ceramic Substrates: A Test Method of Uniform Central Loading and Symmetrical 3-Point Support, Webster Capps, Nat. Bureau of Standards, Washington, D.C. 20234.

TECHNICAL REPORT DISTRIBUTION

<u>Agency</u>	<u>No. of Copies</u>
Director	
Army Materials and Mechanics Research Center	
Watertown, Massachusetts 02172	
ATTN: DRXMR-PL	2
DRXMR-PR	1
DRXMR-CT	1
DRXMR-AP	1
DRXMR-X (Dr. Wright)	1
DRXMR-EO (Dr. Katz)	12
DRXMR-TM (Dr. Lenoe)	2
DRXMR-EO (Dr. Messier)	1
DRXMR-E (Dr. French)	1
DRXMR-P	1
Defense Advanced Research Projects Agency	
1400 Wilson Boulevard	
Arlington, Virginia 22209	
ATTN: Director	1
Deputy Director	1
Deputy Director Materials Sciences	2
(Dr. E. C. van Reuth)	
Technical Information Office	1
(Mr. F. A. Koether)	
Commander	12
Defense Documentation Center	
Cameron Station, Building 5	
5010 Duke Street	
Alexandria, Virginia 22314	

